The measurement of transverse relaxation time (T_2) using histogram from ROI setting in muscle activity study at 1.5 Tesla MRI

Miss Kannikar Kanyakham

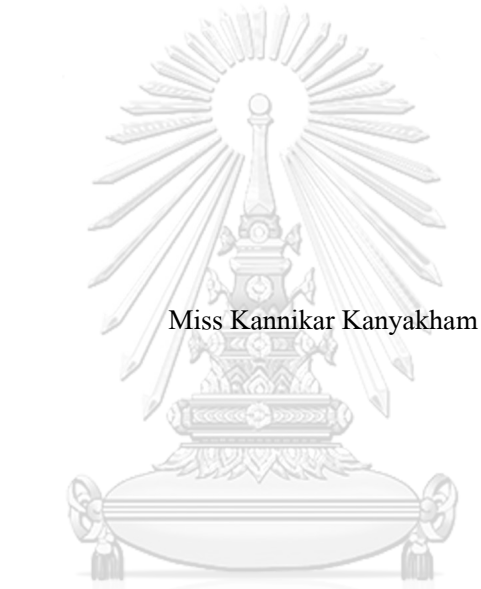

A Thesis Submitted in Partial Fulfillment of the Requirements

for the Degree of Master of Science in Medical Imaging

Department of Radiology

Faculty of Medicine

Chulalongkorn University

Academic Year 2018

การวัดค่าทีทู (T_2 relaxation time) โดยใช้ฮิสโตแกรมจากการวาดบริเวณที่สนใจ (Region of interest) ของกล้ามเนื้อเพื่อการศึกษาการทำงานของกล้ามเนื้อในเครื่องถ่ายภาพสนามแม่เหล็กกำทอน 1.5 เทสลา

น.ส.กรรณิการ์ กัญญาคำ

วิทยานิพนธ์นี้เป็นส่วนหนึ่งของการศึกษาตามหลักสูตรปริญญาวิทยาศาสตรมหาบัณฑิต
สาขาวิชาฉายาเวชศาสตร์ ภาควิชารังสีวิทยา
คณะแพทยศาสตร์ จุฬาลงกรณ์มหาวิทยาลัย
ปีการศึกษา 2561

Thesis Title	The measurement of transverse relaxation time (T_2) using histogram from ROI setting in muscle activity study at 1.5 Tesla MRI
By	Miss Kannikar Kanyakham
Field of Study	Medical Imaging
Thesis Advisor	Associate Professor ANCHALI KRISANACHINDA, Ph.D.
Thesis Co Advisor	Professor Noriyuki Tawara, Ph.D.

Accepted by the Faculty of Medicine, Chulalongkorn University in Partial Fulfillment of the Requirement for the Master of Science

..... Dean of the Faculty of Medicine

(Professor SUTTIPONG WACHARASINDHU, M.D.)

THESIS COMMITTEE

..... Chairman

(Assistant Professor JARTURON TANTIVATANA, M.D.)

..... Thesis Advisor

(Associate Professor ANCHALI KRISANACHINDA, Ph.D.)

..... Thesis Co-Advisor

(Professor Noriyuki Tawara, Ph.D.)

..... Examiner

(Associate Professor Kosuke Matsubara, Ph.D.)

..... External Examiner

(Professor Franco Milano)

กรรณิการ์ กัญญาคำ : การวัดค่าทีทู (T_2 relaxation time) โดยใช้ฮิสโตแกรมจากการวาดบริเวณที่สนใจ (Region of interest) ของกล้ามเนื้อเพื่อการศึกษาการทำงานของกล้ามเนื้อในเครื่องถ่ายภาพสนามแม่เหล็กกำทอน 1.5 เทสลา . (The measurement of transverse relaxation time (T_2) using histogram from ROI setting in muscle activity study at 1.5 Tesla MRI) อ.ที่ปรึกษาหลัก : รศ. ดร.อัญชลี กฤษณจินดา, อ.ที่ปรึกษาร่วม : ศ. ดร.โนริยูกิ ทาวาร่า

การตรวจการทำงานของกล้ามเนื้อด้วยเครื่องถ่ายภาพสนามแม่เหล็กกำทอนเป็นการประเมินสมรรถภาพของกล้ามเนื้อโดยการเปรียบเทียบภาพสนามแม่เหล็กกำทอนระหว่างก่อนและหลังการออกกำลังกาย ซึ่งจะช่วยเพิ่มการหดตัวของกล้ามเนื้อทำให้เกิดการเปลี่ยนแปลงความแตกต่างของความเข้มของสัญญาณภาพทีทู (T_2) การศึกษาก่อนหน้านี้ส่วนใหญ่จะเลือกใช้ลำดับพัลส์มัลติเปิ้ลสปินเอคโค่ (Multiple spin echo: MSE) และวางบริเวณที่สนใจ (ROI) เล็ก ๆ หลายอันในกล้ามเนื้อที่ต้องการวัด ซึ่ง การกำหนดบริเวณที่สนใจ (ROI) ด้วยวิธีนี้ไม่ได้ครอบคลุมกล้ามเนื้อที่ทำการศึกษา ดังนั้นวัตถุประสงค์ของงานวิจัยนี้เพื่อวัดค่าทีทู (T_2) ของกล้ามเนื้อโดยการกำหนดบริเวณที่สนใจให้ครอบคลุมกล้ามเนื้อที่ทำการศึกษาทั้งหมดโดยใช้ค่าเฉลี่ย และค่ากลางของข้อมูลจากฮิสโตแกรมของสัญญาณเพื่อตรวจสอบอิทธิพลของการตั้งค่า ROI ตามลักษณะของฮิสโตแกรมตามสัญญาณเอ็มอาเพื่อศึกษาการทำงานของกล้ามเนื้อในเครื่องถ่ายภาพสนามแม่เหล็กกำทอน 1.5 เทสลา ทำการศึกษาโดยสแกนหุ่นจำลองโดยใช้เครื่องถ่ายภาพสนามแม่เหล็กกำทอน 1.5 เทสลาและใช้ลำดับพัลส์ MSE ร่วมกับค่ารีพิทิชั่นไทม์ (TR) 1,000, 2,000,…4,000 มิลลิวินาที เอคโค่ไทม์ (TE) 15, 30, …, 390 มิลลิวินาทีและต้นขาขวาของอาสาสมัครชายที่มีสุขภาพดีจำนวน 8 คน โดยใช้รีพิทิชั่นไทม์ (TR) 2,000 มิลลิวินาที ตรวจสอบการทำงานของกล้ามเนื้อของอาสาสมัครที่ออกกำลังกายโดยการงอขาและเหยียดขาตรงจำนวน 200 ครั้ง แล้วทำการสแกนต้นขาขวาของอาสาสมัครทั้งก่อนและหลังออกกำลังกาย คำนวณค่าทีทู (T_2) โดยใช้วิธี mono-exponential linear least- squares ของค่า เอคโค่ไทม์ที่ 30, 45, 60, 75 มิลลิวินาที ผลการศึกษาในหุ่นจำลองแสดงให้เห็นว่าเมื่อค่ารีพิทิชั่นไทม์ (TR) เพิ่มขึ้นจำนวนสัญญาณจะเพิ่มขึ้นและกราฟความเข้มของสัญญาณ (SI curve) ของรีพิทิชั่นไทม์ (TR) 1,000 มิลลิวินาทีต่ำกว่าค่าอื่นแต่เมื่อรีพิทิชั่นไทม์ (TR) มีค่า 2,000 มิลลิวินาทีหรือมากว่าสัญญาณที่ได้จะเท่ากัน สำหรับผลการศึกษาการออกกำลังกายได้รับการยืนยันว่าวิธีการใช้ค่าเฉลี่ยในฮิสโตแกรมนั้นเหมือนกับวิธีการทั่วไปกล้ามเนื้อทีทู (T_2) ในทั้งสองวิธีเปรียบเทียบระหว่างการพักผ่อนและหลังการออกกำลังกายค่าทีทู (T_2) มีความแตกต่างอย่างมีนัยสำคัญและยืนยันความแตกต่างของการเพิ่มขึ้นของค่าทีทู (T_2) จากค่าโหมดในฮิสโตแกรม นอกจากนี้การศึกษาการออกกำลังกายยังพบว่ากล้ามเนื้อต้นขาจากการออกกำลังกายด้วยวิธี knee extension พบว่าค่าทีทู (T_2) ของกล้ามเนื้อ RF สูงกว่า VL, VI และ VM ซึ่งแสดงให้เห็นว่านอกจาก RF แล้วผลจากการออกกำลังกายด้วยวิธีนี้ยังส่งผลต่อกล้ามเนื้ออื่นด้วย และการออกกำลังกายด้วยวิธี knee extension มีผลต่อกล้ามเนื้อ VL, VI และ VM เพียงเล็กน้อยจากผลลัพธ์เหล่านี้ยังได้รับการยืนยันว่าผลกระทบของ SNR ของภาพ MR ที่เกิดจากความแตกต่างในการเลือกขดลวดรับสัญญาณรวมถึงการตั้งค่า ROI ที่มีขนาดใหญ่โดยสรุปผลการวิจัยที่ได้รับดังต่อไปนี้ข้อแรกคือการตั้งค่า ROI โดยใช้ฮิสโตแกรมที่เสนอโดยการศึกษานี้สามารถแสดงคุณลักษณะภายในของกล้ามเนื้อตามขอบเขตของความสนใจโดยมีความแปรปรวน (SD) จากการตั้งค่า ROI ลดลง ข้อที่สองคือการเพิ่มขึ้นของทีทู (T_2) หลังจากการออกกำลังกายด้วยวิธี knee extension ไม่เพียงแต่เกี่ยวข้องกับ RF เป็นส่วนใหญ่แต่ยังรวมถึงกล้ามเนื้ออื่นที่ไม่ใช่ RF ด้วยแต่มีส่วนเกี่ยวข้องเพียงเล็กน้อยอิทธิพลต่อทีทู (T_2) ที่คำนวณโดยการตั้งค่า ROI นั้นเกี่ยวข้องกับ SNR เนื่องจากผลกระทบของสัญญาณรบกวน(Noise)ของผลภาพ MR ดังนั้นการวิเคราะห์ทีทูโดยใช้ฮิสโตแกรมจึงมีประโยชน์และสามารถนำไปใช้กับกิจกรรมของกล้ามเนื้อซึ่งไม่ได้รับการยืนยันโดยวิธีการเดิมหรือวิธีทั่วไป (conventional method)

สาขาวิชา	ฉายาเวชศาสตร์	ลายมือชื่อนิสิต .....
ปีการศึกษา	2561	ลายมือชื่อ อ.ที่ปรึกษาหลัก .....
		ลายมือชื่อ อ.ที่ปรึกษาร่วม .....

6074050230 : MAJOR MEDICAL IMAGING

KEYWORD: TRANSVERSE RELAXATION TIME (T2), / MULTIPLE SPIN ECHO (MSE), / REGION OF INTEREST (ROI), MUSCLE FUNCTIONAL MRI(MFMRI)

Kannikar Kanyakham : The measurement of transverse relaxation time (T_2) using histogram from ROI setting in muscle activity study at 1.5 Tesla MRI . Advisor: Assoc. Prof. ANCHALI KRISANACHINDA, Ph.D. Co-advisor: Prof. Noriyuki Tawara, Ph.D.

Muscle functional MRI (mfMRI) is the method to evaluate the muscle activity before and immediately after the muscle exercise by the magnetic resonance images. Exercise of skeletal muscles enhances image contrast in T_2-weighted magnetic resonance (MR) images. In previous studies, the exercised physiology used multiple-spin-echo (MSE) sequences for calculating transverse relaxation time (T_2) with several small regions of interest (ROI) within the target tissue. Such a method may not represent all properties of the target tissue. The purpose of this study is to measure T_2 in rest and exercise muscle at 1.5 Tesla MRI using average mode values in histogram of signal intensity of whole target muscle. A PVA-gel cylindrical phantom was scanned by a 1.5 Tesla whole body MR scanner using MSE with TR 1000, 2000, 3000, 4000 ms, TE 15, 30, ……390 ms, and right thigh of eight healthy male subjects with repetition time (TR) 2000 ms. Subjects performed knee extension exercise of the right thigh 200 times and MR images were acquired at rest and after exercises. T_2 was calculated by mono-exponential linear least-squares of TE 30, 45, 60, 75 ms. Results: for the phantom study, MR signal intensity increases with increasing TR. The SI curve of TR 1000 ms is lower than other TR signals, but the relaxation curve of TR 2000 ms and more show similar MR signals. In exercise study, it has been confirmed that the method using average value in histogram is the same as the conventional method. Muscle T_2 in both methods, rest and after exercise, are significantly different and an increase by combining with the result of mode values from the histogram. In addition, in the muscle activity of quadriceps muscle by knee extension exercise, involvement of other than RF which has not been reported in the past, but in this study, VL, VI, and VM were also confirmed. It could be confirmed that the effect of SNR of MR images caused by the difference in the selection of RF receiver coil as well as the ROI setting is large. In conclusion, the following findings were obtained: first, the ROI setting using histogram proposed by this study can objectively obtain the characteristics within the region of interest with reduced variation. Second, the increase of T_2 after the knee extension exercise is not only involved largely in RF but other muscles also slightly involved. The influence on T_2 calculated by ROI setting is related to SNR because noise of MR image is affected. Therefore, T_2 analysis using histogram is useful and could be applied for muscle activity, which is not confirmed by the conventional method.

Field of Study:	Medical Imaging	Student's Signature .....
Academic Year:	2018	Advisor's Signature .....
		Co-advisor's Signature .....

ACKNOWLEDGEMENTS

The success of this thesis depends on the contribution of many people. First of all, I wish to express the gratitude and deepest appreciation to Associate Professor Anchali Krisanachinda, Ph.D., Department of Radiology, Faculty of Medicine, Chulalongkorn University, my advisor, for her helpful, supervision, guidance, encouragement and polishing of the thesis writing to improve the readability and English expression.

I would like to extremely grateful Professor Noriyuki Tawara, Ph.D., Department of Radiological Sciences, Faculty of Health Sciences, Japan Health Care College, Japan, my co-advisor for his helpful, advice and comment that opened up a new perspective on the MRI research.

I would like to greatly thanks Miss Kanokvalee Ponkanist, M.Sc., Medical Physics staff at Department of Radiology, King Chulalongkorn Memorial Hospital, for her contribute in part of the data collection on the research.

I would like to extremely thanks Associate Professor Sivalee Suriyapee, M.Eng., Division of Radiation Oncology, Department of Radiology, Chulalongkorn University, my teacher for her invaluable advice, constructive comments.

I would like to extremely thank Mr. Taweap Sanghangthum, Ph.D., Division of Radiation Oncology, Department of Radiology, Chulalongkorn University, my teacher for his invaluable advice, constructive comments.

I would like to deeply thank Associate Professor Kosuke Matsubara, Ph.D. from Kanazawa University, Japan and Professor Franco Milano, Ph.D. from University of Florence Italy, External examiner of this thesis defense for their suggestion and teaching in Medical imaging.

I wish to express the deepest appreciation to Assistant Professor Kitiwat Khamwan, Ph.D. for his valuable suggestion to this study.

I would like to thank Mrs. Weeranuch Kitsukjit for her suggestion to this study.

Finally, I am extremely grateful for all lecturers and staffs in the Master of Science Program in Medical Imaging, Department of Radiology, Faculty of Medicine, Chulalongkorn University for their unlimited teaching throughout whole study.

Kannikar Kanyakham

TABLE OF CONTENTS

Page

LIST OF TABLES

Page

Page

LIST OF FIGURES

Page

Page

Page

LIST OF ABBREVIATIONS

ABBREVIATION	TERMS
AAPM	American Association of Physicists in Medicine
ACR	American College of Radiologists
B_0	Magnetic field strength
B_1	Radio-frequency field strength
FID	Free induction decay
FOV	Field of view
FSE	Fast spin echo
mfMRI	Muscle function MRI
MRI	Magnetic resonance imaging
ms	Millisecond
MSE	Multiple spin echo
NSA	Number of signal average
PVA	Polyvinyl alcohol
QC	Quality control
RF	Radiofrequency
RF	Rectus femoris
ROI	Region of interest
SE	Spin echo
T	Tesla

ABBREVIATION	TERMS
T_1	Longitudinal relaxation
T_2	Transverse relaxation
T_2^*	T_2 star
TE	Echo time
TR	Repetition time
TSE	Turbo spin echo
VI	Vastus intermedius
VL	Vastus lateralis
VM	Vastus medialis

CHAPTER I

INTRODUCTION

1.1 Background and rationale

Magnetic resonance imaging (MRI) is a diagnostic imaging technology to determine normal pathological and anatomical images without radiation and being used with increasing in research. In 1988, Fleckenstein et al [1] reported the first phenomenon in subjects that exercise induces MR signal changes resulting primarily from increase in the transverse relaxation time (T_2) as a consequence. Fisher et al [2] suggested that the increases in T_2 could be used as a quantitative measurement for muscle activity, this technique is referred to muscle functional MRI (mfMRI) since Meyer RA et al [3] and/or Ploutz-Snyder LL's report [4].

The mfMRI is an advanced technique to investigate muscle activation patterns associated with various sports by measuring the changes in transverse relaxation time (T_2) of muscle tissue after specific exercise. This technique known as T_2 mapping displays the spatial patterns of muscle recruitment and the intensity of muscle activation immediately after exercise [3, 5]. This activity induces T_2 hyper intensity. Increased T_2 may be partly related to osmotically driven shifts of muscle and water. However, the underlying cellular mechanism for the increase in muscle T_2 during and after exercise is still not fully understood. The phenomenon underlying these mechanisms have been efforts in many MRI studies by T_2 to map the location and relative intensity of whole muscle recruitment during various types of exercise. The accurate measurement of muscle T_2 can affect many MRI applications such as repetition time, echo time, receiving coil selection, and region of interest (ROI) setting, etc. [3, 5-9]

In particular, ROI settings are essential effect on the precision of T_2 calculated by regression analysis. The previous studies in exercised physiology and sports medicine use multiple-spin-echo sequences for calculating T_2 with several region of interests (ROI) selected within the target tissue in the images. This method may not represent all the properties of the target tissue. Therefore, it is necessary to verify T_2 calculated in ROI setting is reflected in the characteristic of the target tissue.

1.2 Research objective

To measure T_2 values in rest and exercise muscle for investigation of the influence of ROI setting based on the characteristics of the histogram of the MR signal at 1.5 Tesla.

1.3 Definition

MRI scanner	MRI scanner is the machine that the magnetic field and radio frequency (RF) signals are used to produce images of anatomical structures, of the presence of disease, and of various biological functions within the human body. MRI produces images that are distinctly different from the images produced by other imaging modalities. The difference is that, MRI does not use radiation (x-rays) and the process can selectively image several different tissue characteristics.
Region of interest (ROI)	ROIs are samples within a data set identified for a particular purpose. The concept of ROI is commonly used in many application areas. The ROI defines the borders of an object under consideration.
Histogram	Represents the actual distribution function of gray values or the numerical data. In the terms of image processing, it is therefore possible to provide the viewer with an entirely black or white image that contains relevant information.
Transverse relaxation time (T_2)	The transverse magnetization generated by applying the RF pulse begins to decay immediately after stopping the application. T_2 relaxation time or transverse relaxation time (T_2) is the time until the transverse magnetization decays to a size of 37%.

CHAPTER II

REVIEW OF RELATED LITERATURE

2.1 Theory

Magnetic resonance imaging (MRI) is a medical imaging process that uses a magnetic field and radio frequency (RF) signals to produce images of anatomical structures, of the presence of disease, and of various biological functions within the human body. MRI produces images that are distinctly different from the images produced by other imaging modalities. The difference is that the MRI process can select image of several different tissue characteristics and pathologic process and produce image contrast, visible in an image because of its effect on other characteristics.

MRI was originally called nuclear magnetic resonance imaging (NMRI). Certain atomic nuclei are able to absorb and emit radio frequency energy when placed in an external magnetic field. In clinical and research MRI, hydrogen atoms are most often used to generate a detectable radio-frequency signal that is received by antennas in close proximity to the anatomy being examined. Hydrogen atoms are naturally abundant in human and other biological organisms, particularly in water and fat. For this reason, most MRI scans essentially map the location of water and fat in the body. Pulses of radio waves excite the nuclear spin energy transition, and magnetic field gradients localize the signal in space. By varying the parameters of the pulse sequence, different contrasts may be generated between tissues based on the relaxation properties of the hydrogen atoms [10].

Atom consists of a nucleus and a shell, which is made up of electrons. In the nucleus, there are protons, that have a positive electrical charge. These protons are constantly turning, or spinning around an axis recall that a moving electrical charge is called a current and that an electrical current generates a magnetic field. Thus, protons have their own magnetic fields and behave like little bar magnets as shown in Figure 2.1[10, 11].

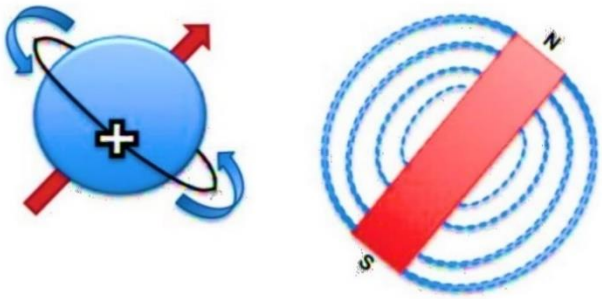

Figure 2.1 Protons possess a positive charge and are constantly spinning around their own axes. This generates a magnetic field making protons similar to bar magnets.

2.1.1 The protons in an external magnetic field.

The magnetic field for each proton is known as a magnetic moment. Magnetic moments are normal randomly orientated as shown in figure 2.2(a). However, when protons are exposed to a strong external magnetic field (B_0), they are aligned in only two ways, either parallel or antiparallel to the external magnetic field as shown in figure 2.2(b). The preferred state of alignment is the one that requires the least energy: that is, parallel to B_0. Accordingly, more protons align with B_0 than against it. The difference in the number of protons aligning parallel and antiparallel to B_0 is typically very small but ultimately depends on the strength of B_0 as well as the temperature of the sample [10, 11].

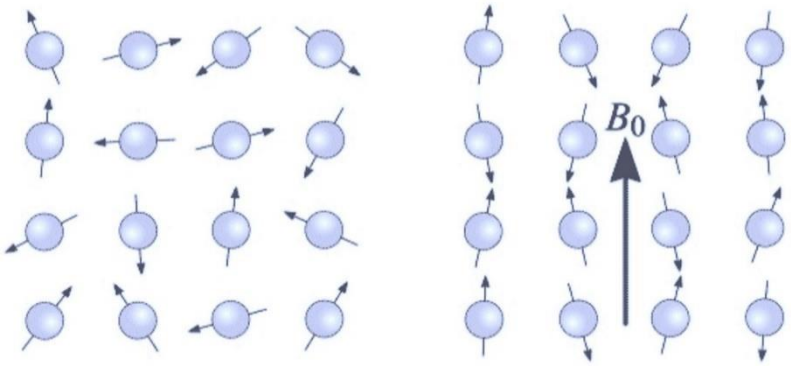

(a) (b)

Figure 2.2 (a) Protons spin with their axes in random directions in the absence of a magnetic field. In the presence of an external magnetic field B_0 (b), the atoms largely align along or against the gradient.

2.1.2 The movement of protons - precession

When put protons in an external static magnetic field, the overall effect on a group of protons (that individually are aligned either parallel or antiparallel to B_0) means that the group of spins classically move in a particular way called precession. Precession can be likened to the movement of a spinning top. When spun, the top wobbles but does not fall over and the axes of the top circles form a cone shape as shown in Figure 2.3. The speed of precession, that is, how many times the protons precess per second, is measured as the precession frequency (also named the Larmor frequency, ω_0, in MHz) and determined by the Larmor equation [10, 12]:

$$\omega_0 = \gamma \cdot B_0$$

ω_0 = Larmor frequency

B_0 = The strength of a magnetic field

γ = Constant, for hydrogen γ is 4257 Hz/T

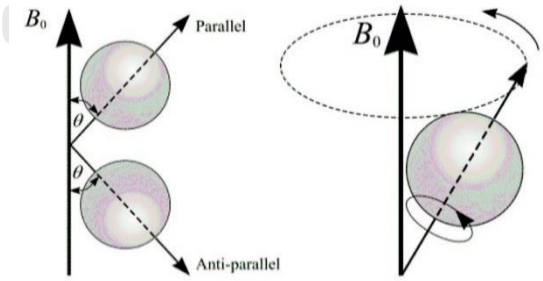

Figure 2.3 The atom precession, proton spinning top around axis of the magnetic field gradient B_0, in the path of a cone.

Protons precess parallel to B_0 and begin to cancel each other out in all directions. The direction of the z-axis, along B_0 Figure 1.4 (a). The result is a sum magnetic field or net

magnetization, often given the symbol M, with the value M_0. It is characteristically shown as a vector. As this sum magnetization parallels the external magnetic field it is also referred to as longitudinal magnetization Figure 2.4 (b).

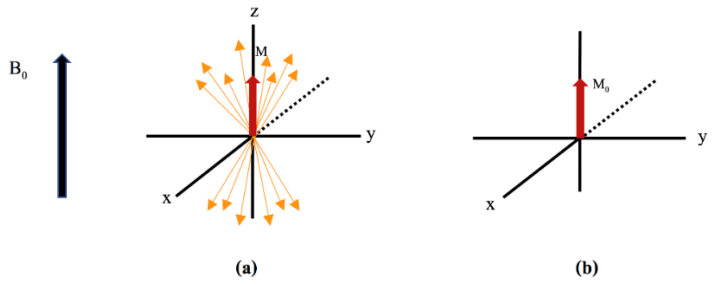

Figure 2. 4 Average of many protons produces the net magnetization M_0

2.1.3 Effect of Radiofrequency Pulses

The net magnetization M can be changed by application, via a coil, of a radiofrequency (RF) pulse applied at the Larmor frequency ω_0. The degree of rotation of the axis M is called the flip angle. This angle is determined by the strength and duration of the RF pulse. A 90˚ pulse moves the direction of M from the z plane into the transverse x-y plane as shown in Figure 2.5 [12].

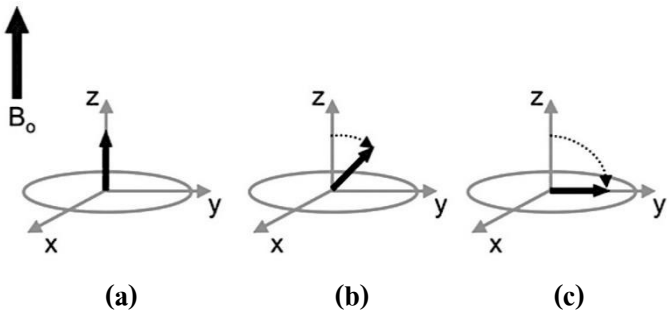

Figure 2.5 Absorption of RF energy. Prior to an RF pulse, the net magnetization (small black arrow) is aligned parallel to the main magnetic field and the z axis. (b, c)

An RF pulse at the Larmor frequency will allow energy to be absorbed by the protons, thus causing the net magnetization to rotate away from the z axis. After transmission of the RF pulse cease, the effective magnetic field returns to B_0. M lies in the x-y plane as shown, and processes about the z axis as shown in Figure 2.6(a). This precession induces a current in a receiving coil,

which the scanner uses to translate an image. As soon as the RF pulse ceases, however, the signal begins to diminish as Mxy *(*where the signal is at its maximum*)* returns to Mz. This free induction decay (FID) as shown in Figure 2.6(b).

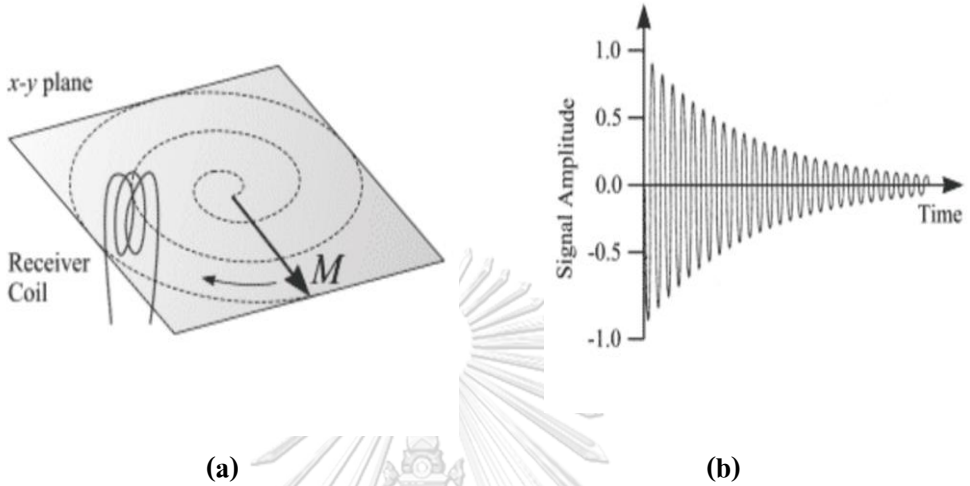

Figure 2.6 (a) After the pulse knocks M into the transverse plane, it rotates about the z axis. (b) The signal, which decreases over time, is detected by the receiver coil.

2.1.4 Magnetization Properties of Tissues

With the patient in the magnet and processing longitudinal magnetization, RF pulses are switched on and off. The purpose of RF pulse is to disturb the protons that proton fall out of alignment with B_0 as shown in Figure 2.5. RF pulses transfer energy to the protons. This can only occur when the RF pulse has the same frequency as the processional frequency of the protons, a phenomenal call resonance; hence the term magnetic resonance imaging. Accordingly, RF pulses are set at the Larmor frequency. The activation of an RF pulse has two main effects on the protons. First, longitudinal magnetization, protons gain energy and move to the higher energy state of being antiparallel to B_0. Second, the RF pulse causes the protons to move in phase (in the same direction, at the same time) with each other rather than in random directions. The result is transvers magnetization in which a new magnetization vector is created in the XY plane and moves in the line with the processing protons at the Larmor frequency [10, 12].

Relaxation occurs in two different ways. Transverse magnetization begins to disappear, a

process called transverse or T_2 relaxation and longitudinal magnetization starts to return to its original value, a process termed longitudinal or T_1 relaxation time.

T_1 Relaxation Time and / or Spin-lattice relaxation time (T_1)

T_1 relaxation time or longitudinal relaxation time (T_1) is the process whereby protons exchange energy with their surroundings to return to their lower energy state and in during cause the restoration of longitudinal magnetization. After a 90° RF pulse rotates the longitudinal magnetization into the transverse plane, this magnetization may be called transverse magnetization. After a 90° RF pulse, the longitudinal magnetization is zero. The magnetization then begins to grow back in the longitudinal direction as shown in Figure 2.7 [11].

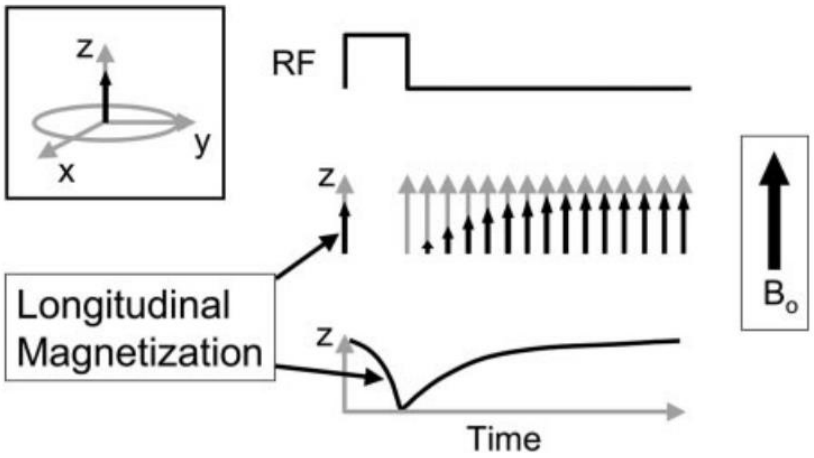

Figure 2.7 Longitudinal (T_1) relaxation. Application of a 90° RF pulse causes longitudinal magnetization to become zero. Over time, the longitudinal magnetization will grow back in a direction parallel to the main magnetic field.

The definition of T_1 is the time required for the longitudinal component of M_Z recovering to 63% of its initial value as shown in the figure 2.8. The magnetization of tissues with different values of T_1 will grow back in the longitudinal direction at different rates as shown in table 2.1.

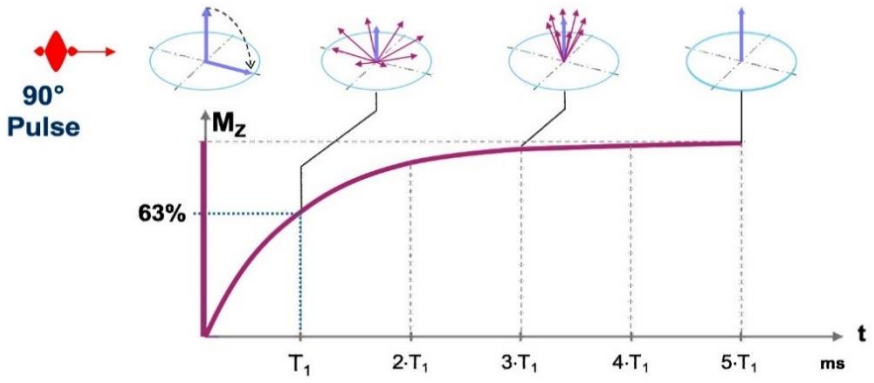

Figure 2. 8 T_1 Relaxation Time

Table 2.1 T_1 for some tissue types at 0.5 Tesla and 1.5 Tesla MRI

Tissue	T_1(ms) at 0.5T	T_1(ms) at 1.5T
Fat	210	260
Liver	350	500
Muscle	550	870
White matter	500	780
Gray matter	650	900
Cerebrospinal fluid	1800	2400

T_2 Relaxation Time and/or Spin-spin relaxation time (T_2)

Transverse relaxation describes the process whereby protons fall out of phase in the x–y plane and transverse magnetization decreases and disappears. There are two causes for this loss of phase coherence.

The first, T_2 relaxation results from slowly fluctuating magnetic field inhomogeneity with in the local tissue. The internal inhomogeneity of spins (protons) influencing other neighboring spins have led to the term spin–spin relaxation also being used for T_2 relaxation.

The second of loss of phase coherence is due to inhomogeneity with in B_0. Magnetic field variations result in slightly different Larmor frequencies for protons at different locations within the field. T_2* (T_2-star) relaxation is the name given to describe the effects that result from the combination of T_2 relaxation and the de-phasing that results from inhomogeneity in B_0. T_2*

relaxation determines the actual rate of decay observed when measuring a free induction decay (FID). The description of T_2 or transverse relaxation begins with the net magnetization aligned with the z direction and a 90° RF pulse that rotates this net magnetization into the transverse plane as shown in Figure 2.9 [11, 12].

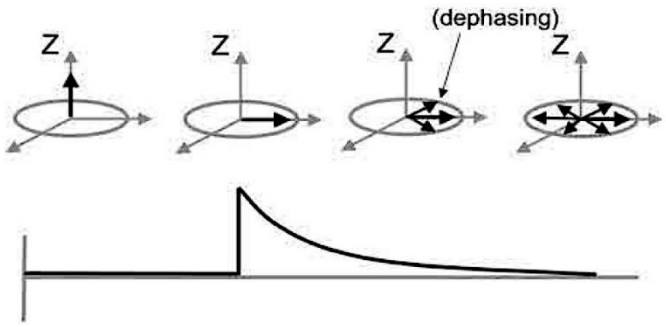

Figure 2.9 Transverse (T_2*) relaxation. Immediately after application of a 90° RF pulse, transverse magnetization is maximized

The transverse magnetization generated by applying the RF pulse begins to decay immediately after stopping the application. The definition of the T_2 relaxation time or transverse relaxation time (T_2) is the time until the transverse magnetization decays to a size of 37% of its initial value as shown in the figure 2.10. Spin–spin interaction governs the speed of T_2 relaxation and hence influences the T_2 values for different tissues [10-12] as shown in table 2.2.

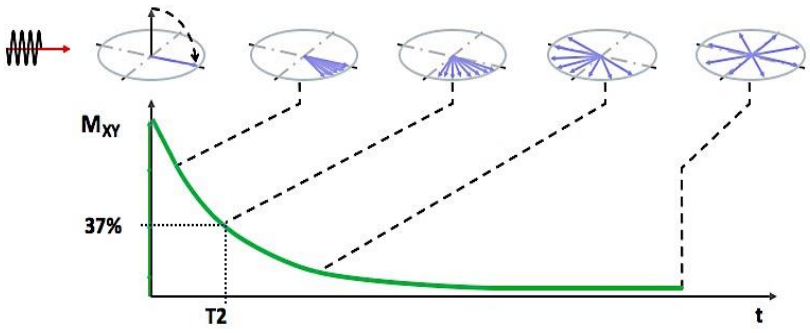

Figure 2.10 T_2 Relaxation Time

The T_2 value for each tissue is unique. T_2 contrast in spin echo imaging: the longer the T_2, the higher the signal.

Table 2. 2 T_2 for some tissue types at 1.5 Tesla MRI

Tissue	T_2 (ms)
Fat	80
Liver	40
Muscle	45
White matter	90
Gray matter	100
Cerebrospinal fluid	160

2.2 Magnetic resonance (MR) Pulse Sequences

2.2.1 Spin Echo (SE)

Spin Echo is the process that uses an RF pulse to produce the echo event such as proton density weighting, T_1 weighting, and T_2 weighting.

The spin echo process

The SE pulse sequence (Figure 2.11) starts with a 90-degree pulse and produces FID that decays according to T_2* ralaxation. After delayed time TE/2, a 180-degree RF pulse inverts the spins that re-establishes phase coherence and produces an echo at a time TE [10, 12].

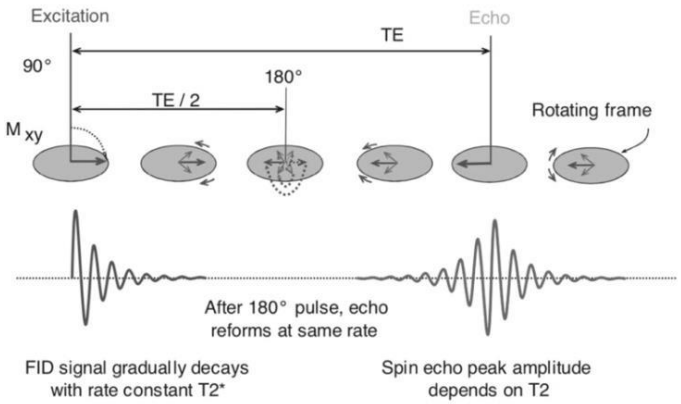

Figure 2. 11 The spin echo process

The timing of RF pulses, the signal formed from these pulses, and the digitization of the signal is shown in Figure 2.12. TE is shown as the time to the echo, and the repetition time is shown as the time it takes to go through the pulse sequence once. This pulse sequence uses a 90° RF pulse with a 180° RF pulse to rephase spins to form an echo. T_1 and T_2-weighted images may be created with this pulse sequence. ADC is analog-to-digital converter; in all pulse sequence diagrams, G is gradient [12].

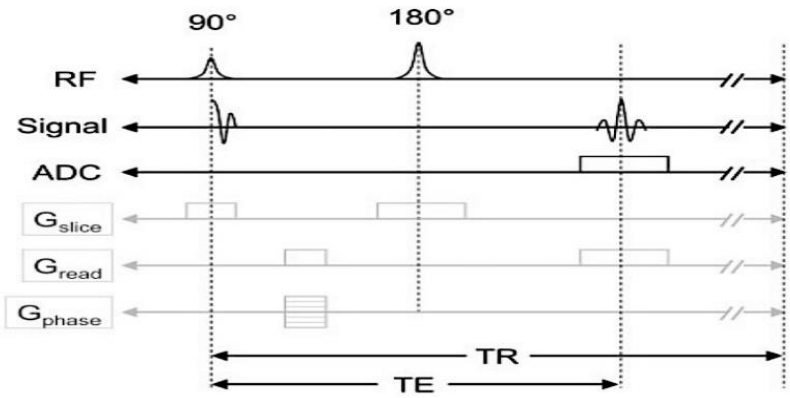

Figure 2. 12 Pulse sequence diagram. A pulse sequence diagram can be used to show the relative timing of certain events during an MR imaging acquisition.

Time of Repetition (TR)

Time of Repetition (TR) is the period from adding the RF pulse (= 90° pulse and/or excitation pulse to adding the next RF pulse. During the TR interval, T_2 decay and T_1 recovery occur in the tissues as show in figure 2.13 [10, 12].

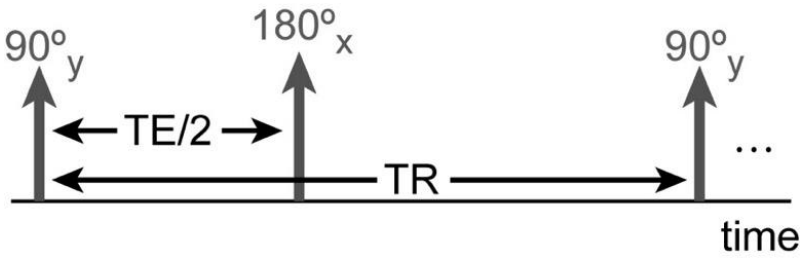

Figure 2. 13 Time of Repetition (TR)

Time of Echo (TE)

The time of echo (TE) is the time between the RF pulse and the appearance of the peak amplitude of an induced echo, which is determined by applying a 180° RF inversion pulse or gradient polarity reversal at a time equal to TE/2. as shown in Figure 2.13

2.2.2 Multiple Spin Echo

Multiple Spin Echo produces a series of echo events within cycles as illustrated in Figure 2.14. This is done by apply several 180° RF pulses after each 90° excitation pulse. The advantage is that echo events with different TE values are produced in one acquisition cycle. Separate images are formed to each TE value [10, 12].

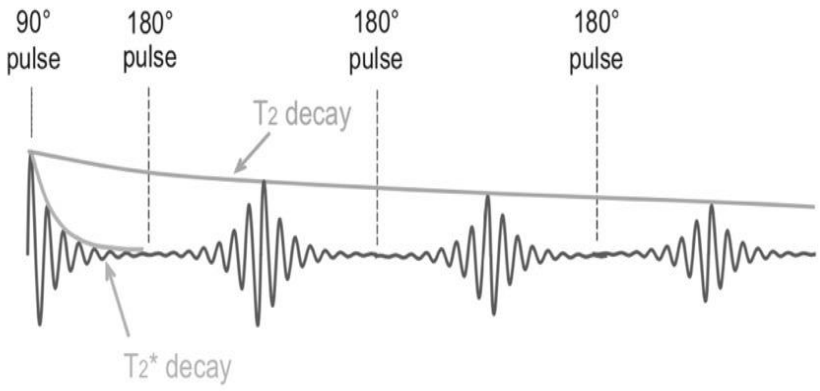

Figure 2. 14 Multiple spin echo imaging

Figure 2.14 T_2 decay is determined from multiple 180° refocusing pulse acquired during the repetition period. While the envelope decays with the T_2* decay constant, the peak amplitudes of subsequent echoes decay exponentially according to the T_2 decay constant, as extrinsic magnetic field inhomogeneity are cancelled.

2.3 Normal anatomy of quadriceps femoris muscle

The quadriceps femoris (QF) muscle is a large muscle group which located in the anterior compartment of the thigh. It is composed of 4 muscle bellies consist of the rectus femoris (RF), which lies in the anterior portion of the thigh; the vastus medialis (VM) and vastus lateralis (VL) on the inner and outer portions, respectively; and the vastus intermedius (VI), which is located posteriorly. The vastus muscles originate from the anterior, medial, and lateral aspects of the femur. The RF originates from the anterior inferior iliac spine (AIIS) as shown in figure 2.15 and figure 2.16 [13].

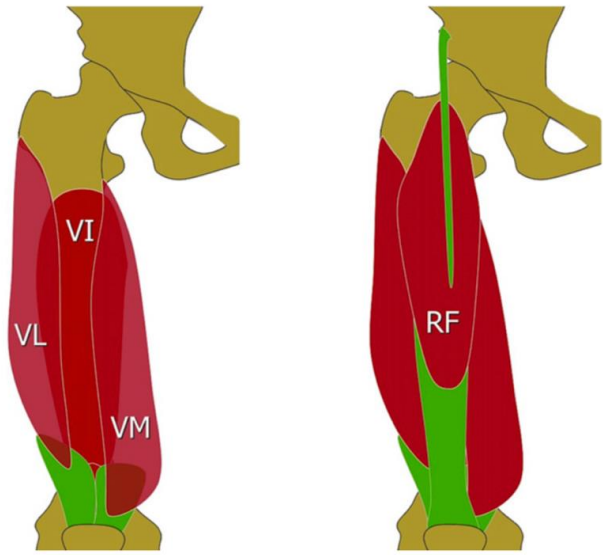

Figure 2. 15 Anatomy of the quadriceps muscle. (a) = deep plane; (b) = superficial plane; VL = vastus lateralis; VI = vastus intermedius; VM = vastus medialis; RF = rectus femoris.

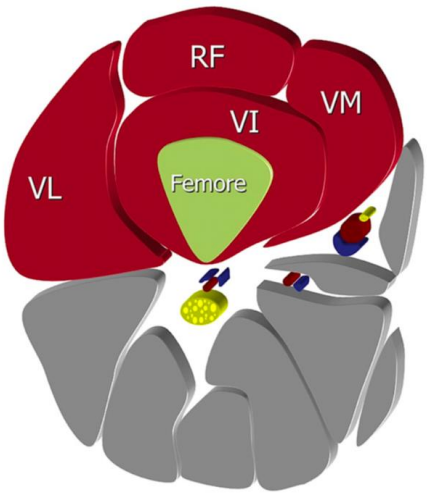

Figure 2. 16 Anatomy of the quadriceps muscle. Axial plane (diagram): VL = vastus lateralis; VI = vastus intermedius; VM = vastus medialis; RF = rectus femoris.

2.4 Review of related literature

Akima H. et al [14] investigated the coordinated activation of individual the quadriceps femoris (QF) muscle during repetitive knee-extension exercises by using muscle functional MRI. They found a moderated correlation between the rectus femoris muscle (RF) and vastus medialis muscle (VM), and between the vastus lateralis muscle (VL) and VM. They also found a strong correlation between the vastus intermedius muscle (VI) and VM, and between the VL and vastus intermedius muscle (VI). They concluded that recruitment of the working muscles is dependent on type of exercise. During repetitive isokinetic knee extension exercise, the rectus femoris muscle is more activated than the other three muscles.

Prior BM. et.al [15] studied the validity of the threshold method for estimating active muscle area by examining the distribution of pixel T_2 in muscles at rest and after moderate vs. intense voluntary exercise. They gave the reason that if the implicit assumption of the threshold method is correct, then the pixel-to-pixel distribution of T_2 should be broadest after moderate exercise, ideally approaching a bimodal distribution, because in that case some motor units (and, therefore, some pixels) would be active while others would not.

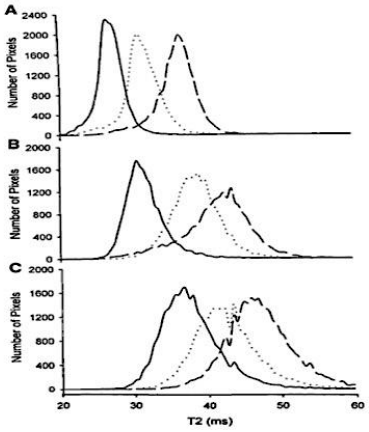

Figure 2. 17 Representative pixel T_2 histograms for biceps brachii (A), Tibialis anterior (B), and quadriceps (c) muscle groups at rest (solid line) and after ½ max (dotted line) and max (dashed line) exercise.

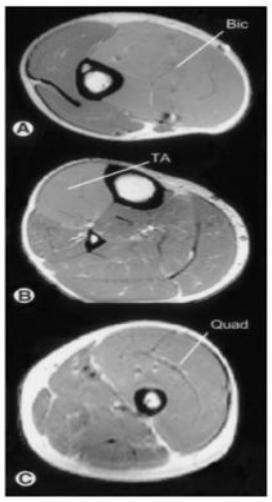

Figure 2. 18 Representative magnetic resonance (MR) images for biceps brachii (Bic, A), tibialis anterior (TA, B), and quadriceps (Quad, C) muscle groups.

After a single repetitive exercise of lifting a weight equal to 50% of previously determined 1 repetition maximum at a rate of 20 repetitions per minute until failure (Max exercise). The mean T_2 of the active muscle also increased slightly with exercise intensity, but the magnitude of this increase was small compared with the T_2 change averaged across the whole muscle. The variation of the pixel-by-pixel T_2 calculation depends on the inherent signal-to-noise ratio (S/N) of the

images, which in turn is a complex function of the ratio of echo time, TE to T_2, the receiver coil's properties, the pixel size and slice thickness, the receiver band- width, and other factors. They suggested that after moderate-intensity exercise, when a muscle is not fully active, the pixel T_2 histogram should substantially broaden, ideally approaching a bimodal distribution. They also found no evidence for such bimodal behavior in the muscles after exercise.

CHAPTER III

RESEARCH METHODOLOGY

3.1 Research design

This study is experimental study that performed in phantom and subjects

3.2 Research design model

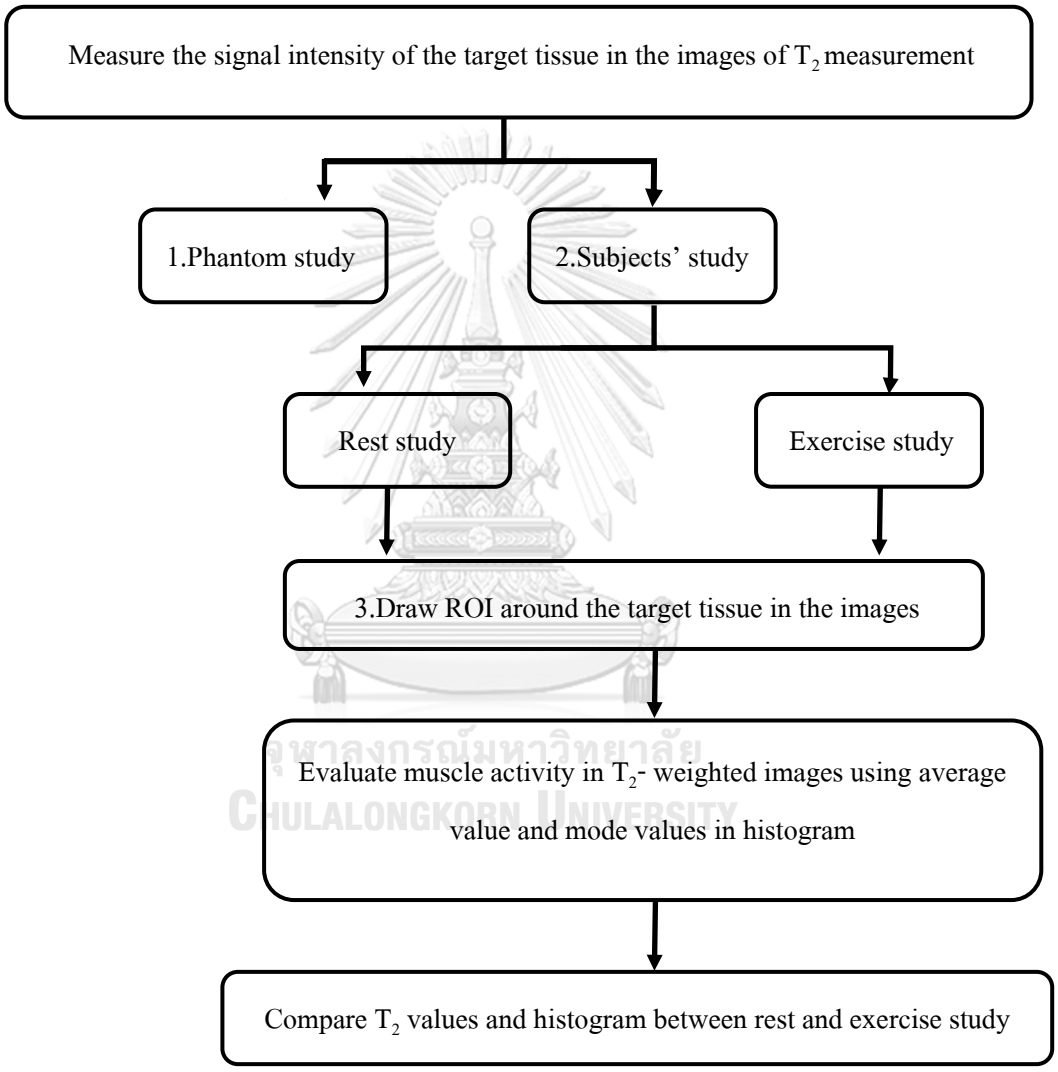

Figure 3. 1 Research design model

3.2.1 Phantom study

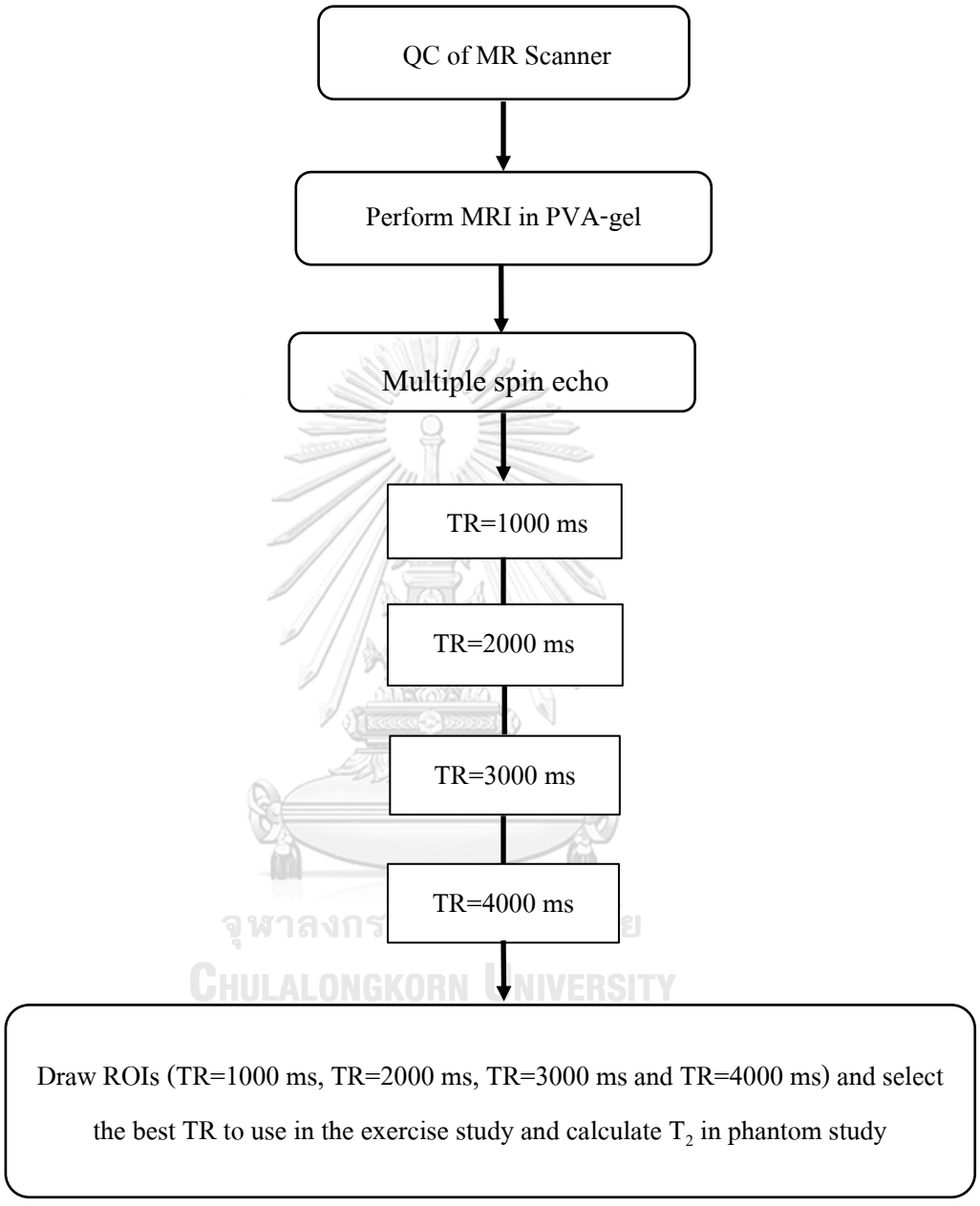

Figure 3. 2 Research design model of phantom study

3.2.2 Subject study

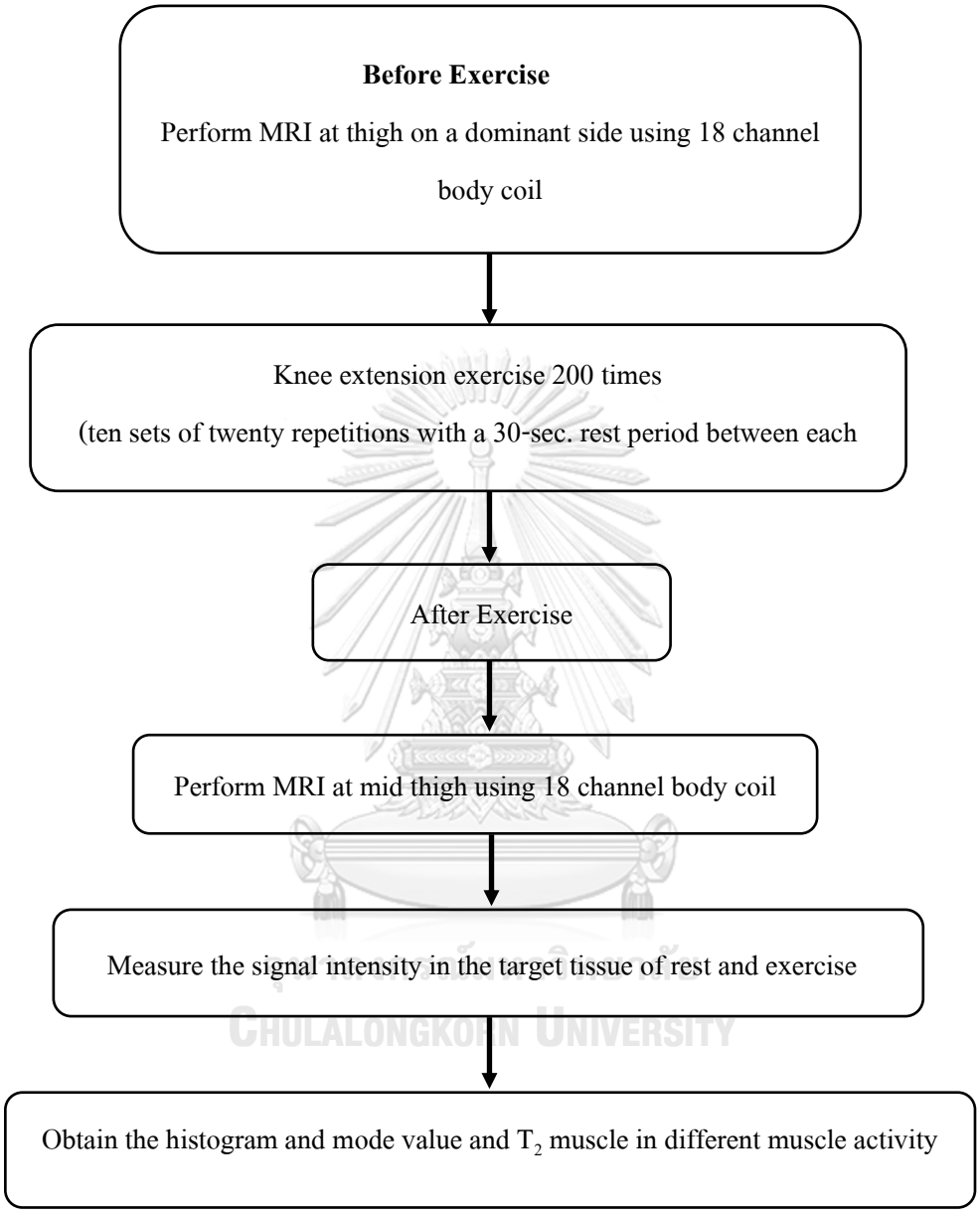

Figure 3. 3 Research design model of subject study

3.3 Conceptual framework

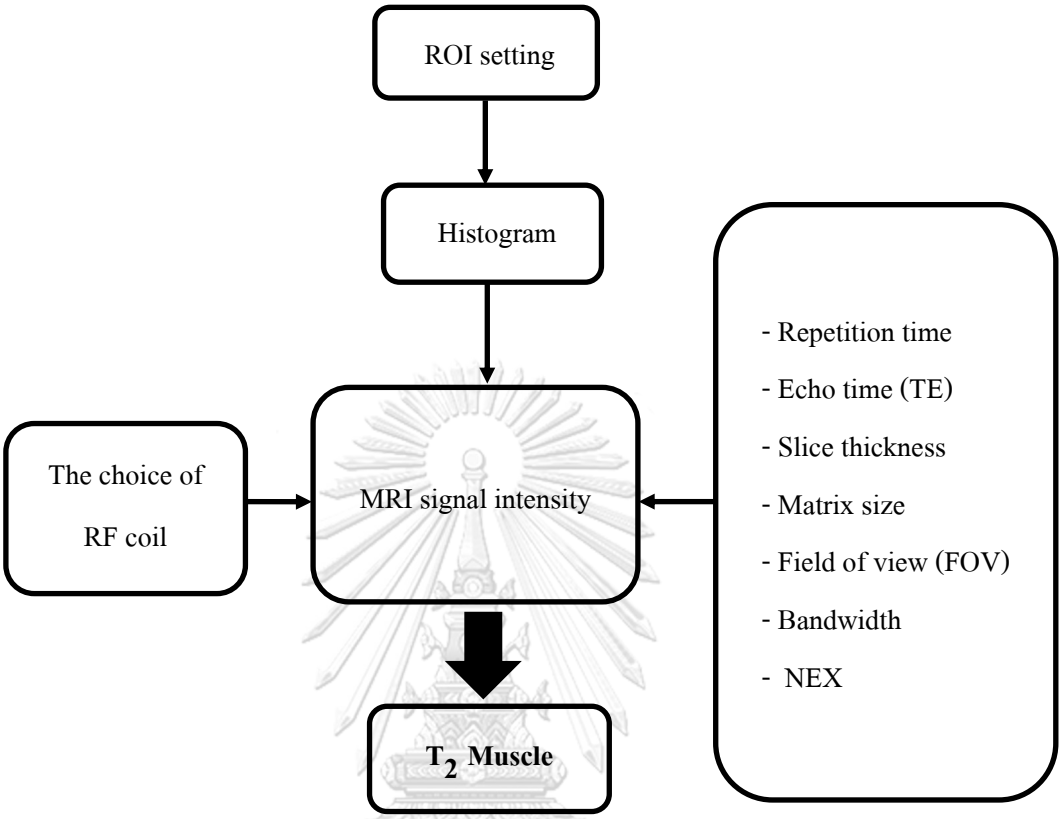

Figure 3. 4 Conceptual framework

3.4 Research question

What are the T_2 values from histogram, using region of interest (ROI) in muscle activity study at 1.5 Tesla MRI?

3.5 The sample

3.5.1 Target population

The healthy male subjects will be recruited based on the following inclusion and exclusion criteria.

3.5.2 Inclusion criteria

- The healthy male volunteer age range 20-35 years old.

- No history of abnormal muscle.
- Male with dominant side.
- Competent to give inform consent.

3.5.3 Exclusion criteria

- Pacemakers, ferromagnetic implants, aneurysm clip in the body
- Claustrophobia and those who cannot perform MRI.
- Unable to exercise as defined.

3.5.4 Sample size determination

The sample population will be determined using this formula

$$N = \frac{(Z_{\alpha/2} + Z_{\beta})^2 \sigma^2}{d^2}$$

- N is Number of subjects in each of two groups
- $Z_{\alpha/2}$ is 95% confidence Interval (1.96) from table
- Z_{β} is corresponding to power 90% (1.282)
- σ^2 is the variance of different in the two groups
- d is the acceptable error

$$N = \frac{(1.96 + 1.282)^2 (2.5)^2}{3^2} = \frac{65.691}{9} = 7.2 \cong 8$$

- N = Number of subjects in each of two group
- $Z_{\alpha/2}$ = 1.96 (2-tailed 0.05 hypothesis test)
- Z_{β} = 1.282 (power = 0.9)
- σ^2 = The variance of different in the two groups
- d = Acceptable error

Need total sample size = 8

3.6 Materials

3.6.1 MRI 1.5 Tesla Whole body scanner, MAGNETOM Aera; Siemens AG, Erlangen, Germany

Figure 3. 5 MRI 1.5 Tesla Whole body scanner, MAGNETOM Aera; Siemens

This MRI scanner model MRI 1.5 Tesla with 70 cm open bore diameter and in combination of All digital-in/digital-out Direct-RF architecture with transmit and receive components at magnet with ultra-short system design installed in 2012 at King Chulalongkorn Memorial Hospital.

3.6.2 Polyvinyl alcohol (PVA)-gel phantom

Figure 3. 6 PVA-gel phantom

A Polyvinyl alcohol gel (PVA-gel) phantom that have T_2 range 80-100 ms. The physical characteristic is approximate of long-term stability and can be used as a reference of human tissue [1, 6].

3.6.3 18-channel Body coil

Figure 3. 7 18-channel Body coil

18-channel design with 18 integrated preamplifiers, with 3 rows of 6 elements each operates in an integrated fashion with the Spine 32. Dual-Density Signal Transfer enables ultra-high-density coil design by integrating key RF components into the local coil.

Quality control (QC)

3.6.4 The 20-channel head/neck phase array coil

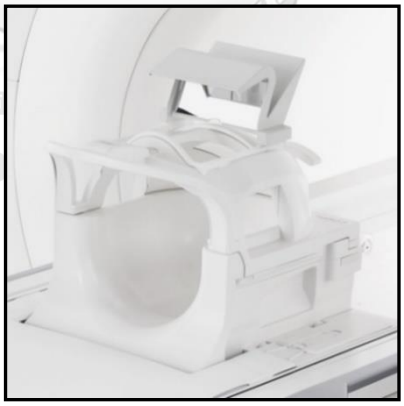

Figure 3. 8 The 20-channel head/neck phase array coil

The 20-channel head/neck phase array coil is the 20-channel design with 20 integrated pre-amplifiers, two rings of 8 elements each and one ring with 4 elements with the Combination coil for head and neck examination for optimized workflow.

3.6.5 ACR MRI accreditation phantom

Figure 3. 9 ACR MRI accreditation phantom

The ACR MRI accreditation phantom is constructed of acrylate plastic, glass, and silicone rubber. Ferromagnetic materials have been excluded. The unit is a cylinder 20.40 cm in diameter by 16.50 cm in length. Internal dimensions are 19.00 cm diameter by 15.00 cm in length. The phantom is filled with 10 millimolar (mmol) nickel chloride solution containing sodium chloride (45 mmol) to simulate biological conductivity. The contrast vial contains 20 mmol nickel chloride and 15 mmol sodium chloride solutions providing a difference in T_1 and T_2 values. Actual values will depend on the field strength in use and the temperature of the phantom [16].

3.7 Method

3.7.1 Quality control (QC) of MRI scanner

Perform QC using head/neck phase array coil 20 channel head/neck following ACR MRI quality control manual 2015.

3.7.2 Phantom study

Position PVA-gel phantom with 18-channel body array coil at the center alignment of the magnetic field. The protocol was MSE pulse sequence with using parameter protocol by following table 3.1

Parameter protocol of phantom

Table 3. 1 The protocol used for phantom study on different TR

Parameter protocol	Multiple spin echo (MSE)
Repetition time (ms)	4TRs (1,000, 2,000…, 4,000)
Echo time (ms)	26 TEs (15, 30, 45, …, 390)
Matrix size	256 x 256
Flip angle (deg)	N/A
Bandwidth (Hz/Px)	N/A
Acquisition time (min)	4:20, 8:36, 12:53, 17:10
Slice thickness (mm)	5
FOV (mm^2)	200 x 200
Number of excitations	1

3.7.3 Subjects' study

Eight healthy male subjects (mean age ± SD = 26.88 ± 5.10 years; mean height ± SD = 171.00 ± 5.20 cm; mean body weight ± SD = 72.63 ± 5.60 kg) were performed MR imaging at the level of intermediate of thigh. Set the pulse sequence acquisition parameters as in table 3.2. All Subjects were fully informed of the procedures to be used as well as the purpose and risk of the study, and written informed consent was obtained.

Before Exercise

1. Position the thigh on the dominant side of male with body coil at the center alignment of the magnetic field.

2. Perform MRI at the middle of the thigh using multiple spin echo pulse sequence and set repetition time by select from phantom study that the suitable repetition time. (short scan time, high SNR)

3. Regarding ROI setting, draw ROI for measurement of the signal intensity and calculate T_2 value. The anatomy of muscle is approved by the radiologist.

Exercise study

Exercise of the thigh on a dominant side. Perform the knee extension by lying and slowly extend the knee, until leg is fully extended, then return to the start, subject exercises 200 times.

After exercise

Perform MRI at the thigh 5 minutes after exercise by using parameter protocol as before exercise.

Table 3. 2 Parameter protocol of subject study

Parameter protocol	Multiple spin echo (MSE)
Repetition time (ms)	TR 2000
Echo time (ms)	26 TEs (15, 30, 45, …, 390)
Matrix size	256 x 256
Flip angle(deg)	N/A
Bandwidth (Hz/Px)	N/A
Acquisition time (min)	4:20, 8:36, 12:53, 17:10
Slice thickness (mm)	5
FOV (mm^2)	250x250
Number of excitations	1

3.7.4 Data analysis

MR images were transferred to a personal computer for image analysis. Signal intensity (SI) was determined from MR images using Image J version 1.47 (NIH, USA; http://rsb.info.nih.gov/ij/). Muscle T_2 was calculated from reconstructed T_2- images on a pixel by pixel using mono-exponential linear least squares methods of four TEs, TE = 30, 45, 60, 75 ms. First for the phantom study, four region of interests (ROIs) were placed on PVA-gel image at the center core of the image (Figure 3.10 a) that is conventional method and set single large ROI at the center core of the image (Figure 3.10 b). Second, for subjects' study, four ROIs were created within the target tissue that is conventional method as shown in Figure 3.10 (c) and ROI created around whole target muscle on rectus femoris (RF), vastus lateralis (VL), vastus intermedius (VI) and

vastus medialis (VM) that are whole muscle method (Figure 3.10 d) to obtain the average values and employ the histogram.

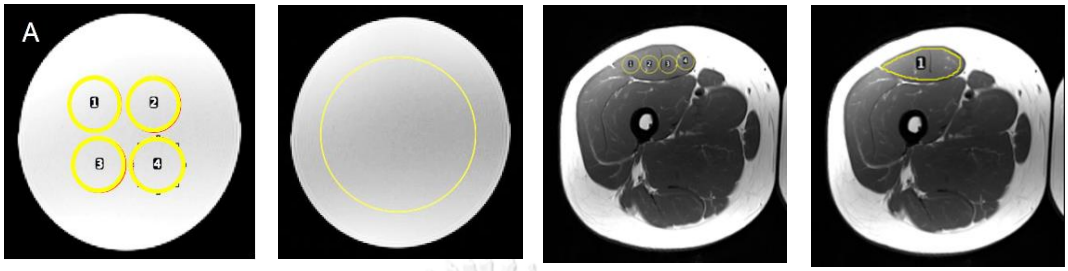

(a) **(b)** **(c)** **(d)**

Figure 3. 10 Representative of ROI created within the PVA-gel phantom (a), (b) and axial MR image of right thigh at RF muscle (c), (d).

T_2 were calculated using a nonlinear least-square curve fitting as a mono-exponential function. The Y of T_2-weighted images was modelled on an exponential decay with increasing TE as follows:

$$Y(TE) = Y_{TE=0} \times \exp(-\frac{TE}{T_2})$$

Where,

$Y_{TE=0}$ is the SI at TE = 0, and the unknown coefficient is $Y_{TE=0}$ and T_2.

3.8 Statistical analysis

3.8.1 Statistical analysis of phantom

The results of T_2 comparison exceeding 10 percent were assumed to be significantly different. Reference form the previous studies concluded that relaxation times (T_1 and T_2) within the majority of the biological range can be estimated by MRI with an overall accuracy of 5 to 10 percent [17]. The wide spread in relaxation time measurement is due to real variations and not a lack precision.

3.8.2 Statistical analysis of subjects

This study is experimental study performed in phantom and subjects to determine: Maximum, Minimum, Mean, SD, Mode and Histogram of T_2.

3.8.2.1 The one-sided t-test was used to determine the statistical difference between the T_2 at rest and after exercise; $P<0.05$ was considered significant.

3.8.2.2 SPSS version 22 and Excel will be used to analyze the data.

3.9 Outcome measurement

Measurement variables

- Independent variables: setting ROI
- Dependent variables: Signal intensity, T_2

T_2 relaxation time is calculated from rate of signal intensity

3.10 Expected benefit

Obtain T_2 values of quadriceps femoris muscles (QF) in healthy male volunteer, age range 20-35 years old for evaluation of the muscle function during exercise in Sport Medicine.

3.11 Ethical consideration

This study is performed in phantom and in healthy male by measurement the signal intensity and setting the ROI in MR images using histogram and mode value for study muscle activity at 1.5 Tesla MRI. The research proposal was submitted to the Ethic Committee, Faculty of Medicine Chulalongkorn University for approval. The participants received the adequate information about the study before signing a consent form at King Chulalongkorn Memorial Hospital and each participant decided whether or not to participate as research subjects. The participant can refuse participation at any time.

Add Belmont

Respect for persons

Respect for free and informed consent: Participants will receive adequate information about the study before signing a consent form and have the right to refuse participation at any time.

Respect for confidential: Researchers will maintain the confidentiality of the volunteer records in no identifiable data of participants.

Beneficence/Non-maleficence

Potential risks to the participants are protected by a check list for screening before and after perform MRI. There is the protective equipment to avoid skin contact with the coil directly and a device used to reduce noise.

Justice

The Justice is a clear inclusion and exclusion criteria, non-bias

3.12 Limitation

The forces of exercise study in each subject are different

CHAPTER IV

RESULTS

4.1 Quality control of MRI scanner

The quality control of 1.5 Tesla MRI system was performed by following the ACR manual (2015). The results of quality control of MRI scanner were illustrated in table 4.1

Table 4. 1 Report of MRI 1.5 Tesla performance test

Location	King Chulalongkorn Memorial Hospital
Date	30 March 2018
Manufacturer	Siemens Healthcare
Model	MAGNETOM Aera 1.5 Tesla installed 2012
Series number	52058
Software version	Syngo MR E 11
PASS	Geometric Accuracy
PASS	High Contrast Spatial Resolution
PASS	Slice Position Accuracy
PASS	Slice Thickness
PASS	Image Uniformity
PASS	Signal to Noise Ratio
PASS	Low Contrast Detectability
PASS	Magnet Visual Inspection
PASS	**Overall Phantom Test Results**

4.2 Phantom study

In phantom study: Figure 4.1 shows the T_2 relaxation curve of the PVA-gel phantom from histogram data use average values.

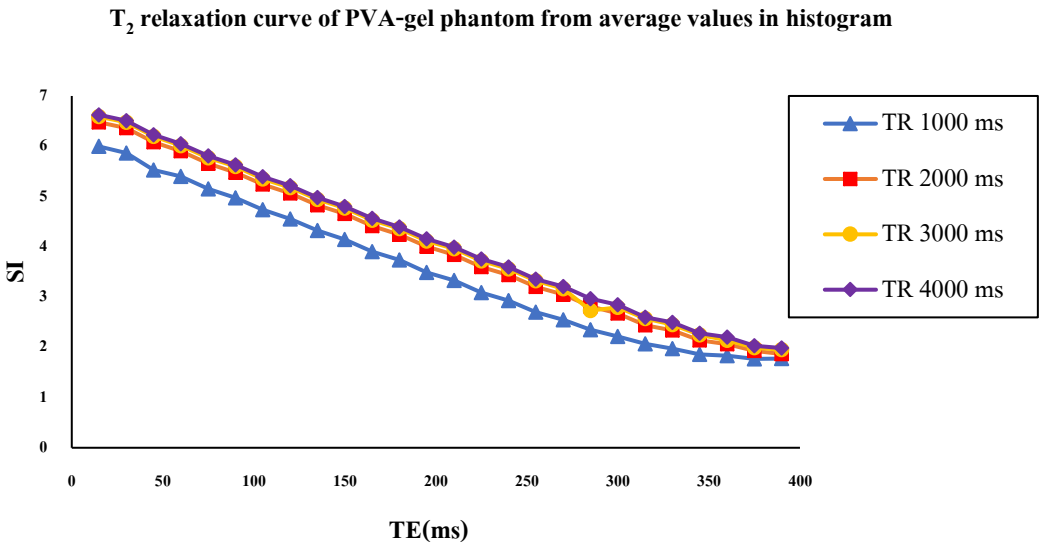

Figure 4. 1 T_2 relaxation curve of PVA-gel phantom from average values in histogram

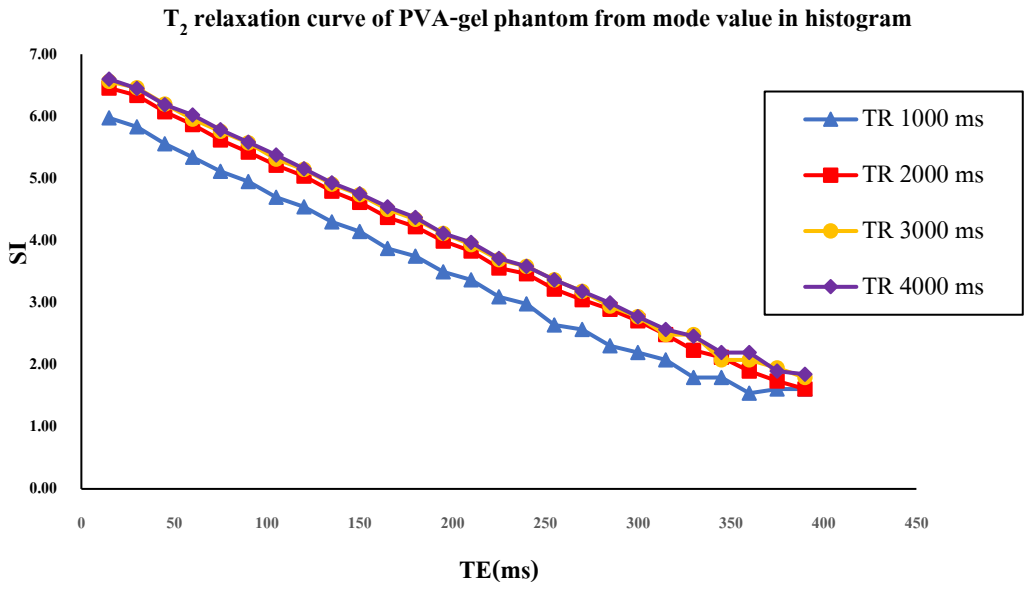

Figure 4. 2 T_2 relaxation curve of PVA-gel phantom from mode values in histogram

From Figure 4.1 and Figure 4.2 MR signal of PVA-gel phantom increase with increasing TR. The SI curve of TR 1000 ms is lowest among than the other TR's signals. The relaxation curve when TR is 2000 ms or more, tended to show approximately the same MR signal. T_2 of PVA-gel phantom, TR 2000 ms calculated by use average value from histogram data by average values T_2 = 65.36 ms and mode value T_2 = 70.42 ms.

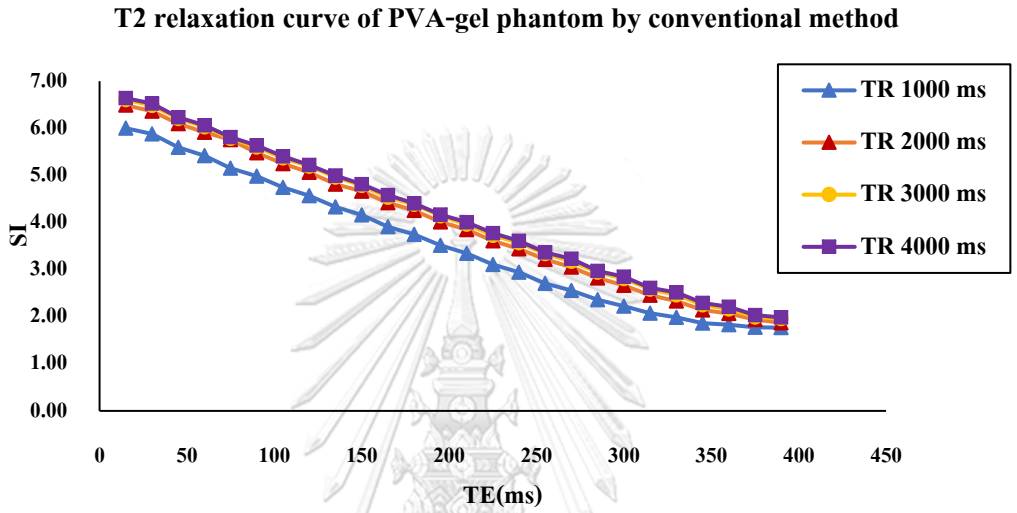

Figure 4. 3 T_2 relaxation curve of PVA-gel phantom from conventional method

Figure 4.3 T_2 relaxation curve of PVA-gel phantom by conventional method, MR signal increases with increasing TR as the same T_2 relaxation curve by using average and mode values from histogram data.

Table 4. 2 T_2 of PVA- gel phantom by conventional method and histogram data by using average value versus the percent different values in each TR.

ROI setting	T_2 (ms)			
	TR 1000 ms	TR 2000 ms	TR 3000 ms	TR 4000 ms
Conventional method	69.44 ± 5.22	69.93 ± 4.74	71.42 ± 2.55	71.42 ± 0.53
Histogram (average value)	71.43 ± 3.03	70.92 ± 0.00	69.93 ± 0.65	70.92 ± 1.34
% Difference	0.01	0.74	1.26	3.22

Table 4. 3 T_2 of PVA- gel phantom by conventional method and histogram data by using mode value versus the percent different values in each TR.

	T_2 (ms)			
ROI setting	TR 1000 ms	TR 2000 ms	TR 3000 ms	TR 4000 ms
Conventional method	66.01 ± 5.22	64.88 ± 4.74	64.41 ± 2.55	64.04 ± 0.53
Histogram (mode value)	63.43 ± 0.23	63.86 ± 1.72	64.52 ± 0.00	67.73 ± 4.12
% Difference	3.90	1.57	0.17	5.76

Although T_2 data acquisition conditions are the same, it is reported that data obtained due to causes such as differences between devices have an error of about 10 percent. The results of T_2 comparison exceeding 10 percent difference are assumed to be significantly different [17]. In these results, the results of comparison method are not significantly different in each TR from table 4.2.

4.3 Subjects' study

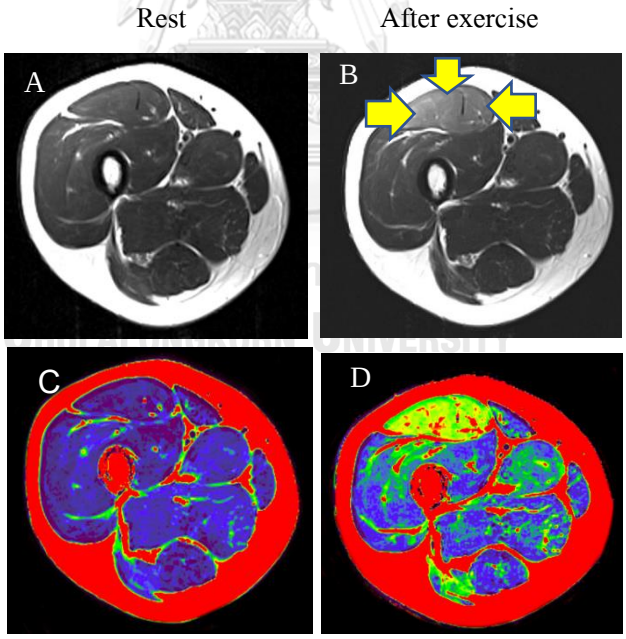

Figure 4. 4 T_2-weighted MR images (A, B) and T_2 map images (C, D) of the right thigh at rest and after exercise. In colored T_2 map, when muscle T_2 becomes high, it changes from blue to green, yellow.

In Figure 4.4, T_2-weighted images of the right thigh as shown in image A is muscle at rest and B is after exercise. The arrows indicated the area of activated muscle and color reconstructed T_2 map. Image C and D show an apparent muscle activation difference between rest and after exercise, rest is blue color and after exercise, the blue color changes to the green and yellow color.

Table 4. 4 T_2 of subjects' study from eight healthy male volunteers at rest of rectus femoris (RF), vastus lateralis (VL), vastus medialis (VM) and vastus intermedius (VI) calculated by using average values from histogram data.

Subject No.	T_2 (ms)			
	Rest			
	RF	VL	VI	VM
1	33.04	35.42	34.88	33.15
2	33.57	32.44	35.94	35.38
3	31.61	31.62	31.35	31.10
4	33.75	33.78	33.45	34.29
5	33.37	35.08	35.17	33.86
6	31.38	32.47	34.68	34.41
7	32.68	33.82	36.50	33.60
8	33.68	36.00	35.93	35.81
Mean ± SD	32.89 ± 0.35	33.83 ± 0.45	34.74 ± 0.32	33.95 ± 0.39

Table 4. 5 T_2 of subjects' study from eight healthy male volunteers at after exercise of rectus femoris (RF), vastus lateralis (VL), vastus medialis (VM) and vastus intermedius (VI) calculated by using average values from histogram data.

Subject No.	T_2 (ms)			
	After exercise			
	RF	VL	VI	VM
1	50.60	37.42	43.53	37.94
2	45.52	33.45	38.56	35.71
3	37.88	34.17	34.17	34.56
4	49.26	34.09	35.26	34.73
5	38.46	35.35	37.22	37.04
6	42.68	33.83	37.45	35.38
7	42.86	34.88	36.64	33.71
8	42.20	37.21	37.04	36.10
Mean ± SD	43.68 ± 0.85	35.05 ± 0.50	37.48 ± 0.69	35.65 ± 0.77

Table 4. 6 T_2 of subjects' study from eight healthy male volunteers at rest and after exercise of rectus femoris (RF), vastus lateralis (VL), vastus medialis (VM) and vastus intermedius (VI) calculated by using average values from histogram data.

Muscle	Histogram data (average values)		Statistical difference between T_2 of rest and after exercise
	T_2 (ms)		
	Rest	After exercise	P-value
RF	32.89 ± 0.35	43.68 ± 0.85	< 0.01
VL	33.83 ± 0.45	35.05 ± 0.5	0.03
VI	34.74 ± 0.32	37.48 ± 0.69	0.02
VM	33.95 ± 0.39	36.65 ± 0.77	0.03

Table 4. 7 T_2 of subjects' study from eight healthy male volunteers at rest of rectus femoris (RF), vastus lateralis (VL), vastus medialis (VM) and vastus intermedius (VI) calculated by using mode values from histogram data.

Subject No.	T_2 (ms)			
	Rest			
	RF	VL	VI	VM
1	33.00	34.50	32.82	36.00
2	31.25	32.00	31.00	32.00
3	30.00	30.00	30.00	30.00
4	31.00	31.75	32.00	31.00
5	32.94	31.68	34.77	31.48
6	32.12	33.67	33.44	34.38
7	31.00	33.90	32.00	32.00
8	32.00	32.79	33.71	32.25
Mean ± SD	31.66 ± 0.25	32.54 ± 0.39	32.47 ± 0.16	32.39 ± 0.26

Table 4. 8 T_2 of subjects' study from eight healthy male volunteers at after exercise of rectus femoris (RF), vastus lateralis (VL), vastus medialis (VM) and vastus intermedius (VI) calculated by using mode values in histogram.

Subject No.	T_2 (ms)			
	After exercise			
	RF	VL	VI	VM
1	51.00	35.21	47.31	36.00
2	50.30	32.00	33.00	32.00
3	34.00	31.00	31.00	32.00
4	46.00	33.00	32.00	31.75
5	41.04	32.90	42.44	32.05
6	43.89	35.21	34.56	40.49
7	42.00	35.21	36.10	32.00
8	42.07	34.01	32.91	32.30
Mean ± SD	43.79 ± 0.83	33.29 ± 0.87	36.17 ± 1.36	33.57 ± 0.16

Table 4. 9 T_2 of subjects' study from eight healthy male volunteers at rest and after exercise of rectus femoris (RF), vastus lateralis (VL), vastus medialis (VM) and vastus intermedius (VI) calculated by using mode values in histogram.

Histogram data (mode values)		
Muscle	T_2 (ms)	
	Rest	After exercise
RF	31.66 ± 0.25	43.79 ± 0.83
VL	32.24 ± 0.39	33.90 ± 0.87
VI	32.47 ± 0.16	36.17 ± 1.36
VM	32.39 ± 0.26	33.57 ± 0.16

Table 4. 10 T_2 of subjects' study from eight healthy male volunteers at rest of rectus femoris (RF), vastus lateralis (VL), vastus medialis (VM) and vastus intermedius (VI) calculated by using average values from conventional method.

Subject No.	T_2 (ms)			
	Rest			
	RF	VL	VI	VM
1	34.29	34.65	36.03	34.33
2	34.24	35.59	33.81	31.21
3	31.04	32.23	31.32	30.89
4	32.90	32.71	31.22	32.14
5	34.90	34.55	33.21	30.84
6	32.19	31.17	32.01	34.12
7	32.28	32.49	32.86	32.21
8	33.57	33.40	33.94	33.72
Mean ± SD	33.18 ± 1.73	33.35 ± 1.54	33.05 ± 2.11	32.43 ± 1.75

Table 4. 11 T_2 of subjects' study from eight healthy male volunteers at after exercise of rectus femoris (RF), vastus lateralis (VL), vastus medialis (VM) and vastus intermedius (VI) calculated by using average values from conventional method.

Subject No.	T_2 (ms)			
	After exercise			
	RF	VL	VI	VM
1	51.40	36.33	41.78	35.84
2	46.00	35.69	34.38	33.11
3	36.75	32.74	32.19	39.25
4	49.32	36.13	31.97	34.15
5	39.90	34.29	35.19	34.98
6	43.36	35.10	34.59	34.78
7	43.72	34.10	32.99	32.38
8	40.82	35.02	36.08	37.21
Mean ± SD	43.91 ± 1.82	34.92 ± 2.43	34.89 ± 1.99	35.21 ± 2.56

Table 4. 12 T_2 of subjects' study from eight healthy male volunteers at rectus femoris (RF), vastus lateralis (VL), vastus medialis (VM) and vastus intermedius (VI) calculated by using average values from conventional method.

Conventional method			Statistical difference between T_2 of rest and after exercise
	T_2 (ms)		
Muscle	Rest	After exercise	P-value
RF	33.18 ± 1.73	43.91 ± 1.82	< 0.01
VL	33.35 ± 1.54	34.92 ± 2.43	0.02
VI	33.05 ± 2.11	34.89 ± 1.99	0.02
VM	32.43 ± 1.75	35.21 ± 2.56	0.02

From table 4.9 and table 4.12, the paired t-test was used to determine the statistical difference between T_2 at rest and after exercise; T_2 calculated by use average value from histogram data tends to be slightly higher than the conventional method. RF, VL, VI and VM after exercise confirmed the significantly difference of T_2 in both methods. In addition, the result of statistical analysis was confirmed to be a difference as an increase by combining with the result of mode values from the histogram.

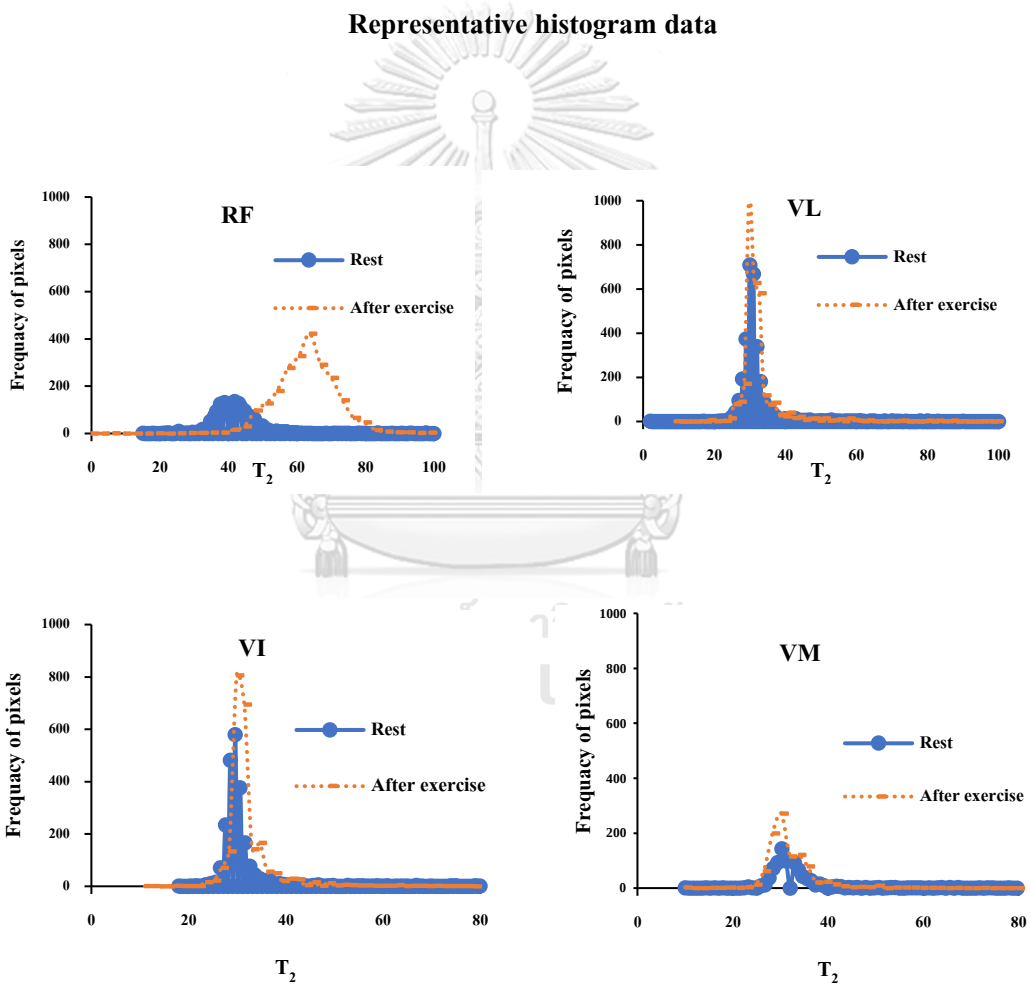

Figure 4. 5 Representative histogram data of T_2 for RF, VI, VM and VL at rest and after exercise.

Table 4. 13 Compare T_2 relaxation of eight subjects at rest of rectus femoris (RF), vastus lateralis (VL), vastus medialis (VM) and vastus intermedius (VI) between conventional and whole muscle method (mode and average values in histogram).

Rest	T_2 (ms)			
ROI Setting	RF	VL	VI	VM
Conventional	33.18 ± 1.73	33.35 ± 1.54	33.05 ± 2.11	32.43 ± 1.75
Whole muscle (our method)	32.89 ± 0.35	33.83 ± 0.39	34.74 ± 0.32	33.95 ± 0.39
% Difference	0.87	1.44	5.11	4.69

Table 4. 14 Compare T_2 relaxation of eight subjects at after exercise of rectus femoris (RF), vastus lateralis (VL), vastus medialis (VM) and vastus intermedius (VI) between conventional and whole muscle method (mode and average values in histogram).

After exercise	T_2 (ms)			
ROI Setting	RF	VL	VI	VM
Conventional	43.91 ± 1.82	34.92 ± 2.43	34.89 ± 1.99	35.21 ± 2.56
Whole muscle (our method)	43.68 ± 0.85	35.05 ± 0.50	37.48 ± 0.69	36.65 ± 0.77
% Difference	0.52	0.38	7.42	4.09

From the table 4.13 and table 4.14 the comparison between conventional and whole muscle method are show in the same way as phantom study (TR 2000 ms) muscle T_2 of quadriceps muscle are not significantly different. The results of T_2 comparison exceeding 10 percent difference are assumed to be significantly different [17].

CHAPTER V

DISCUSSION AND CONCLUSIONS

5.1 Discussion

The mfMRI is a non-invasive technique showing exercise enhances image contrast among induced skeletal muscles in T_2- weighted magnetic resonance (MR) images. Most previous studies in exercised physiology use MSE sequences for calculating transverse relaxation time (T_2) with several regions of interest (ROI) selected within the target tissue in the images. Such the method may not represent all the properties of the target tissue. The purpose of this study is to measure T_2 values in rest and exercise muscles for investigation of the influence of ROI setting based on the characteristics of the histogram of the MR signal at 1.5 Tesla using average values in histogram of signal intensity by setting ROI around the whole target muscle.

5.1.1 Phantom study

MR signal increases with increasing TR. The SI curve of TR 1000 ms is lower than the other TR's signals because a short TR offers low SNR according to an incomplete recovery of longitudinal magnetization. However, the relaxation curves of TR 2000 ms and more are similar MR signals. In order to detect changes of MR signal that induced exercise in more detail in the analysis of muscle activity using MRI, the acquiring time of MR images as short as possible is desirable. It is suggested that TR at 2000 ms is reasonable from the relationship between MR signal change due to incomplete recovery of longitudinal magnetization and the optimization to reduce the acquiring time. From the previous study, Thomsen C. et al [17] reported that device-to-device variation of data acquired by imaging under the same conditions occurs within 10%, T_2 of each TR in conventional method and histogram data using average values and mode values are not significantly different.

5.1.2 Subjects' study

For exercise study, in the statistical test, one-sided t-test was used to determine the statistical difference between the T_2 at rest and after exercise; $P<0.05$ was considered significant.

Regarding the conventional method using high SNR MR images in exercise study, an increasing T_2 was confirmed for a slight muscle activity RF, VL, VI and VM and similar to the previous studies [14]. The results also confirmed with VL, VM, and VI during repetitive knee extension exercise in average value and mode from histogram. RF is more activated than the VL, VI, and VM and similar to conventional method in Akima report [14]. Many studies reported that T_2 of muscular activity of the quadriceps muscle induced by knee extension exercise was obviously increasing in RF. In this study, T_2 of VL, VM, and VI were slightly increasing after muscle activity by the effect of SNR of MR images using the RF phase array coil (18 channel body coil). Therefore, a slight muscle activity is expected to be new finding for clarifying the physiological mechanism of muscle activity induced exercise. The results confirmed that T_2 of quadriceps muscle at rest, and after exercise was a normal distribution. The conventional method and histogram, T_2 of quadriceps muscle at after exercise was significantly higher than T_2 at rest but SD of histogram showed a lower value. Therefore, it was suggested that the variance in ROI influences the extraction result in the conventional method.

The results of this study show that the image noise always affects both the setting method of ROI and the calculation process of T_2, and it is necessary to eliminate the influence as much as possible.

5.2 Conclusions

T_2 analysis using average and mode values from histogram of quadriceps muscle, by using average value at rest and after exercise, RF=32.89, 43.68, VL=33.83, 35.05, VI=34.74, 37.48, VM=33.95, 36.65 ms and using mode value, RF=31.66, 43.79, VL=32.24, 33.90, VI=32.47, 36.17, VM=32.39, 33.57 ms respectively. It was confirmed that the increase of T_2 after the knee extension exercise is not only obviously increasing in RF but also slightly increasing in VL, VI, VM after muscle activity. The ROI setting using histogram proposed by this study, can objectively obtain the characteristics within the region of interest with reduced variation.

Therefore, T_2 analysis using histogram is useful and could be applied for muscle activity, which is not confirmed by the conventional method.

REFERENCES

1. Blechinger J, Madsen E, Frank GJMp. Tissue‐mimicking gelatin–agar gels for use in magnetic resonance imaging phantoms. 1988;15(4):629-36.

2. De Smet AA, Fisher DR, Heiner JP, Keene JSJSr. Magnetic resonance imaging of muscle tears. 1990;19(4):283-6.

3. Meyer RA, Prior BMJESSR. Functional magnetic resonance imaging of muscle. 2000;28(2):89-92.

4. Ploutz-Snyder LL, Yackel-Giamis EL, Rosenbaum AE, Formikell MJTJoGSABS, Sciences M. Use of muscle functional magnetic resonance imaging with older individuals. 2000;55(10):B504-B11.

5. Cagnie B, Elliott J, O'Leary S, D'hooge R, Dickx N, Danneels LJjoo, et al. Muscle functional MRI as an imaging tool to evaluate muscle activity. 2011;41(11):896-903.

6. Tawara N, Itoh AJMRiMS. Effects of MR image noise on estimation of short T2 values from T2-weighted image series. 2007;6(4):187-97.

7. Ray CA, Dudley GAJJoAP. Muscle use during dynamic knee extension: implication for perfusion and metabolism. 1998;85(3):1194-7.

8. Kinugasa R, Kawakami Y, Fukunaga TJMri. Quantitative assessment of skeletal muscle activation using muscle functional MRI. 2006;24(5):639-44.

9. Stoller DW. Magnetic resonance imaging in orthopaedics and sports medicine: Lippincott Williams & Wilkins; 2007.

10. Bushberg JT, Boone JM. The essential physics of medical imaging: Lippincott Williams & Wilkins; 2011.

11. Hendrick REJR. The AAPM/RSNA physics tutorial for residents. Basic physics of MR imaging: an introduction. 1994;14(4):829-46.

12. Currie S, Hoggard N, Craven IJ, Hadjivassiliou M, Wilkinson IDJPmj. Understanding MRI: basic MR physics for physicians. 2013;89(1050):209-23.

13. Pasta G, Nanni G, Molini L, Bianchi SJJou. Sonography of the quadriceps muscle: examination technique, normal anatomy, and traumatic lesions. 2010;13(2):76-84.

14. Akima H, Takahashi H, Kuno S-y, Katsuta SJEjoap. Coactivation pattern in human quadriceps during isokinetic knee-extension by muscle functional MRI. 2004;91(1):7-14.

15. Prior BM, Foley JM, Jayaraman RC, Meyer RAJJoAP. Pixel T2 distribution in functional magnetic resonance images of muscle. 1999;87(6):2107-14.

16. Chen C-C, Wan Y-L, Wai Y-Y, Liu H-LJJodi. Quality assurance of clinical MRI scanners using ACR MRI phantom: preliminary results. 2004;17(4):279-84.

17. Kjær L, Thomsen C, Henriksen O, Ring P, Stubgaard M, Pedersen EJAR. Evaluation of relaxation time measurements by magnetic resonance imaging: a phantom study. 1987;28(3):345-51.

APPENDICES

Appendix A: Data record form

Table A. 1 Data record form for phantom study

Study: Phantom study Date:				
TE	Signal Intensity (Mean ± SD)			
	TR (ms)			
	1000	2000	3000	4000
15				
30				
45				
60				
75				
90				
105				
120				
135				
150				
165				
180				
195				
210				
225				
240				
255				
270				
285				
300				
315				
330				
345				
360				
375				
390				

Table A. 2 Record T_2 of phantom study in different TR

Pulse Sequences	T_2 (ms)			
	TR 1000 ms	TR 2000 ms	TR 3000 ms	TR 4000 ms
Mean ± SD				

Table A. 3 Subject information of subject study.

Subject NO.	Age (Years)	Body Weight (cm.)	Height (kg.)
1			
2			
3			
4			
5			
6			
7			
8			
Mean ± SD			

Table A. 4 Mean signal intensity in each TE of in subject study.

Study: Exercise Study	
Study Date:	
Center/Room:	
Subject No.	
Thigh (dominant side) ☐ Right side ☐ Left side	
☐ Rest	☐ After Exercise
	Signal Intensity (Mean± SD)
TE	TR = _____ (TR from Phantom study)
15	
30	
45	
60	
75	
90	
105	
120	
135	
150	
165	
180	
195	
210	
225	
240	
255	
270	
285	
300	
315	
330	
345	
360	
375	
390	

Table A. 5 T_2 of subjects' study at rest and after exercise study of rectus femoris (RF), vastus intermedius (VI), Vastus medialis (VM) and vastus lateralis (VL)

Subject No.	T_2 (ms)							
	Rest				After exercise			
	RF	VI	VM	VL	RF	VI	VM	VL
1								
2								
3								
4								
5								
6								
7								
8								

Table A. 6 Average of T_2 at rest and after exercise of rectus femoris (RF), vastus intermedius (VI), vastus medialis (VM) and vastus lateralis (VL)

Muscle	T_2 (ms)	
	Rest	After exercise
Rectus femoris (RF)		
Vastus intermedius (VI)		
Vastus medialis (VM)		
Vastus lateralis (VL)		

Appendix B: Quality control of MRI scanner

The Quality Control Program of MRI scanner use ACR protocols for scan two phantoms on routine clinical head protocol. The scan parameters for localizer and the first 2 axial series of image refer to ACR sequences or ACR images.

1. Phantom set-up and alignment for scanning

1. Position an ACR phantom in head coil, the word "NOSE" is where the nose would be for a standard head study and the word "CHIN" is where the chin would be located in a standard head study.
2. The center of the phantom should be place in the center of the head coil and aligned with the positioning indicator light at the center alignment of the magnetic field.

2. Scanning the phantom

- A sagittal locator sequence should be acquired with the acquisition parameters listed on the Site Scanning Data Form.

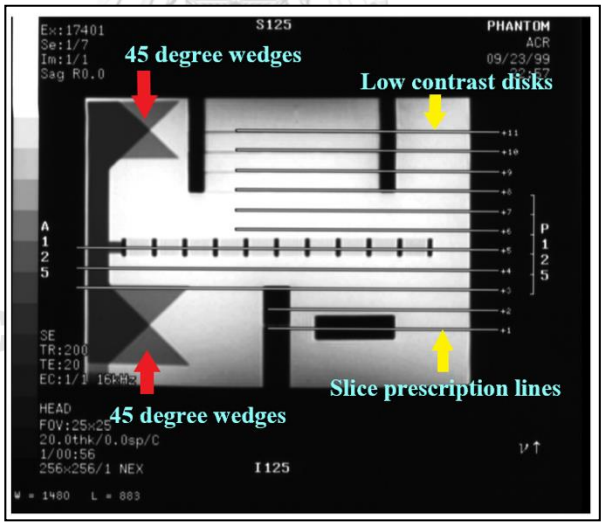

Figure B. 1 Sagittal localizer view of ACR MRI Phantom with slice locations for transaxial scans indicated.

- The sagittal locator scan should result in an image similar to Figure B.1. If the pairs of 45° crossed wedges are not visible in the scan, the phantom must be repositioned and rescanned.
- A horizontal line used for slice prescription should be parallel to the low contrast disks

located at the top of head coil. If not, the phantom must be repositioned.

- The next two scan acquisitions are transaxial pulse sequences acquired with identical spatial parameters follow the table B.1.
- At least 11 slices should be obtained, aligned using graphic prescription from the sagittal locator as shown in Figure B.1.

Table B. 1 Pulse Sequence Acquisition Parameters

Series	Sequence	TR msec	TE msec	FOV mm	Thick mm	Gap mm	NEX	Matrix
ACR T_1	SE	500	20	250	5	5	1	256 x 256
ACR T_2	SE	2000	20/80	255	5	5	1	256 x 288
Clinical Brain T_1	SE	525	12	220	5	0	1	256 x 255
Clinical Brain T_2	TSE	3989	100	250	6	1	1	255 x 256

Quantitative tests

1. Geometric Accuracy
2. High contrast spatial resolution
3. Slice Thickness Accuracy
4. Slice position accuracy
5. Image intensity uniformity
6. Percent signal ghosting
7. Low contrast object Detectability
8. Image Artifact Evaluation
9. Magnet Visual Inspection

1. Geometric Accuracy

Purpose: To assess the accuracy of the image lengths in the imaged subject. A failure means that dimensions in the images differ from the true dimensions substantially more than ± 2 mm.

Methods: 1. Display the localizer, measure the end-to-end length of the phantom as it appears in the localizer (line No.1) as shown in figure B.2.

2. Display slice 1 of the ACR T_1 series. Measure the diameter of the phantom in 2 directions: top-to-bottom (line No.2) and left-to-right (line No.3).

3. Display slice 5 of the ACR T_1 series. Measure the diameter of the phantom in 4 directions: top-to-bottom (line No.4), left-to-right (line No.5)

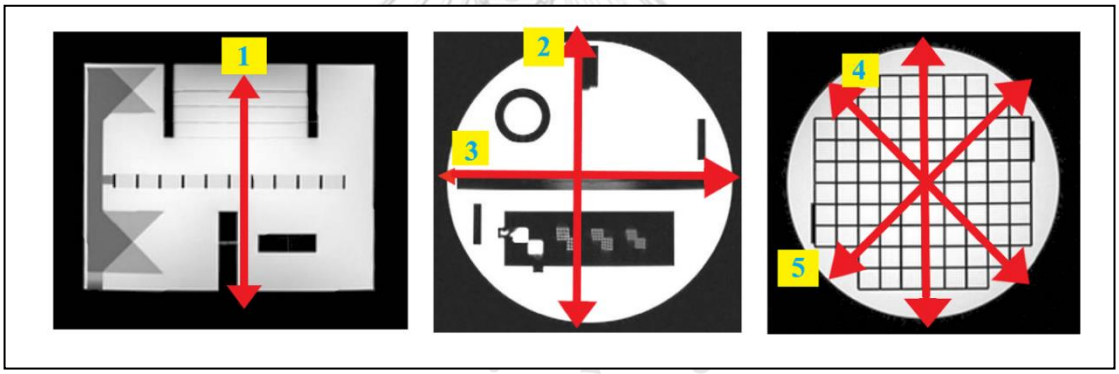

Figure B. 2 The end to end length and diameter measurement illustrated of the phantom

Table B. 2 Geometric accuracy test results used ACR protocols

Line No.	True Value (mm)	Sag Locator		ACR T_1		ACR T_2 _TE20		ACR T_2 _TE80	
		Meas. (mm)	Diff (mm)	Meas. (mm)	Diff (mm)	Meas. (mm)	Diff (mm)	Meas. (mm)	Diff (mm)
1	148.00	148.00	0	-	-	-	-	-	-
2	190.00	-	-	191.12	+1.12	189.60	-0.40	190.81	+0.81
3	190.00	-	-	189.73	-0.27	189.43	-0.57	189.89	-0.11
4	190.00	-	-	190.80	+0.80	190.48	+0.48	191.02	+1.02
5	190.00	-	-	190.60	+0.60	189.95	-0.15	190.27	+0.27

Results of Geometric accuracy

Table B. 3 Geometric accuracy test results used routine protocols

Lie No.	True Value (mm)	**Sag Locator**		**Clinical T_1**		**Clinical T_2**	
		Meas. (mm)	Diff (mm)	Meas. (mm)	Diff (mm)	Meas. (mm)	Diff (mm)
1	148.00	148.00	0	-	-	-	-
2	190.00	-	-	191.67	+1.67	191.25	+1.25
3	190.00	-	-	189.97	-0.03	190.26	+0.26
4	190.00	-	-	190.64	+0.64	191.34	+1.34
5	190.00	-	-	190.26	+0.26	190.25	+0.25

Recommended Action Criteria: +/- 2 mm in all planes.

Comment: PASS

2. High contrast spatial resolution

Purpose: To assess the scanner's ability to resolve small objects when the contrast-to-noise ratio is sufficiently high.

Methods: 1. Display the slice

2. Magnify the image by a factor of between 2 and 4, keeping the resolution insert visible in the display. This is illustrated in Figure B.3.

3. Begin with the leftmost pair of hole arrays, which is the pair with the largest hole size, 1.1 mm.

4. Look at the rows of holes in the UL array, and adjust the display window and level to best show the holes as distinct from one another.

5. If all 4 holes in any single row are distinguishable from one another, score the image as resolved right- to-left at this particular hole size.

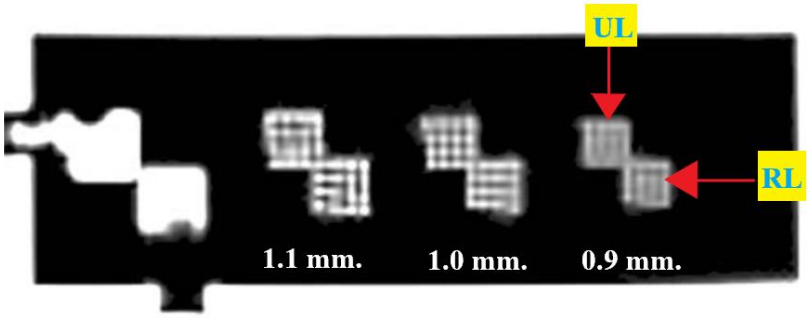

Figure B. 3 Magnified portion of slice 1 displayed appropriately for visually assessing high contrast resolution.

Results of High Contrast Spatial Resolution test

Table B. 4 Results of High Contrast Spatial Resolution test

Series	Spatial Resolution (mm)		Result
	UL	RL	
ACR Axial T_1	1.0	1.0	PASS
ACR Axial T_2	1.0	1.0	PASS
Clinical Axial T_1	1.0	1.0	PASS
Clinical Axial T_2_TE 20	1.0	1.0	PASS
Clinical Axial T_2_TE 80	1.0	1.0	PASS

Recommended Action Criteria: 1 mm or smaller

Comment: PASS

3. Slice Thickness Accuracy

Purpose: To assess the accuracy of a slice of specified thickness. The prescribed slice thickness is compared with the measured slice thickness.

Methods: 1. For each ACR series, the length of the signal ramps in slice 1 is measured according to the following procedure:

2. Display slice 1, and magnify the image by a factor of 2 to 4. Adjust the display level so that the signal ramps are well visualized. The ramp signal is much lower than surrounding water.

3. Place a rectangular ROI at the middle of each signal ramp as shown in Figure B.4. Note the mean signal values for each of these 2 ROIs then average those 2

values together. The result is a number approximating the mean signal in the middle of the ramps.

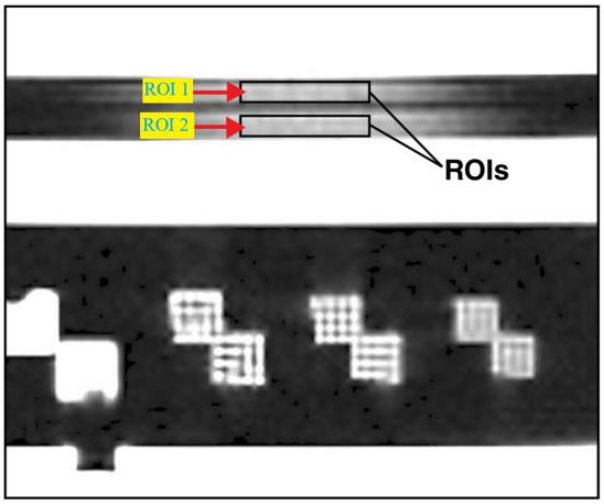

Figure B. 4 ROIs placed for measuring average signal in the ramps.

4. Display level to half of the average ramp signal calculated. Use the on-screen length measurement tool of the display station to measure the lengths of the top and bottom ramps. Record these lengths.

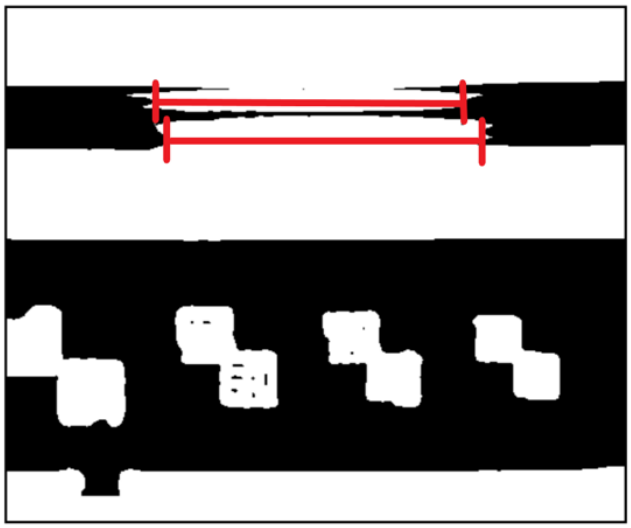

Figure B. 5 Magnified region of slice 1 showing slice thickness signal ramps

5. The slice thickness is calculated using the following formula

Slice thickness = 0.2 x (top x bottom) / (top + bottom)

Results

Table B. 5 Slice Thickness Accuracy

Series	Slice Thickness Setting (mm)	Slice Thickness Measurement (mm)	Difference (mm)	Result
ACR T_1	5	5.18	+0.18	Pass
ACR T_2_TE 20	5	5.28	+0.28	Pass
ACR T_2_TE 80	5	5.41	+0.41	Pass
Clinical T_1	5	5.58	+ 0.58	Pass
Clinical T_2	5	5.62	+0.62	Pass

Recommended Action Criteria: The measured thickness should be 5.0 ±0.7mm (4.3-5.7 mm)

Comment: PASS

4. Slice position accuracy

Purpose: To assesses the accuracy with which slices can be prescribed at specific locations utilizing the localizer image for positional reference.

Methods: Slice position accuracy test the differences between the prescribed and actual positions of slices 1 and 11 are measured. These measurements are made for the ACR T_1 and T_2 series. The slices 1 and 11 are prescribed so as to be aligned with the vertices of the crossed 45° wedges at the inferior and superior ends of the

phantom respectively. On slices 1 and 11 the crossed wedges appear as a pair of adjacent, dark, vertical bars at the top (anterior side) of the phantom. For both slice 1 and slice 11, if the slice is exactly aligned with the vertex of the crossed wedges, then the wedges will appear as dark bars of equal length on the image. By design of the wedges, if the slice is displaced superiorly with respect to the vertex, the bar on the observer's right (anatomical left will be longer. If the slice is displaced inferiorly with respect to the vertex, the bar on the left will be longer.

Measurements are made for slices 1 and 11 of the ACR T_1 and ACR T_2 series. Use the following procedure for each image:

1. Display the slice. Magnify the image by a factor of 2 to 4, keeping the vertical bars of the crossed wedges within the displayed portion of the magnified image.

2. Adjust the display window so the ends of the vertical bars are well defined and use the on-screen length measurement tool to measure the difference in length between the left and right bars. The length to measure is indicated by the arrows in Figure B6.

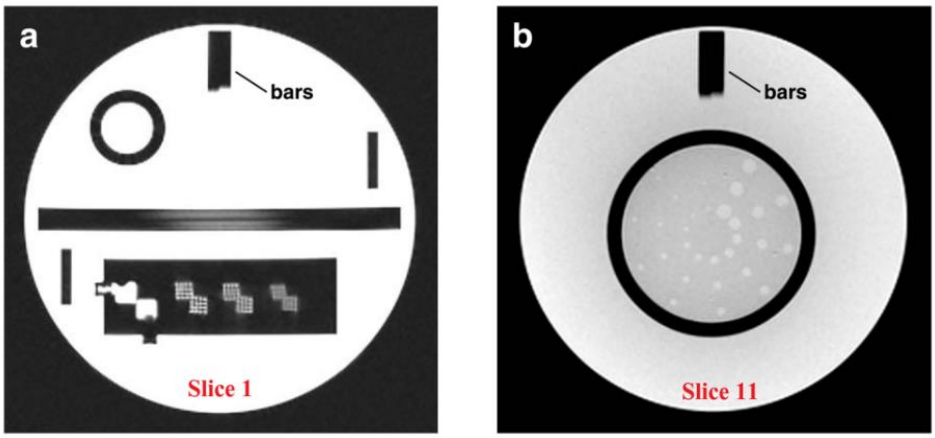

Figure B. 6 Images of slice 1 (a) and slice 11 (b)with the pairs of vertical bars from the 45° crossed wedges indicated.

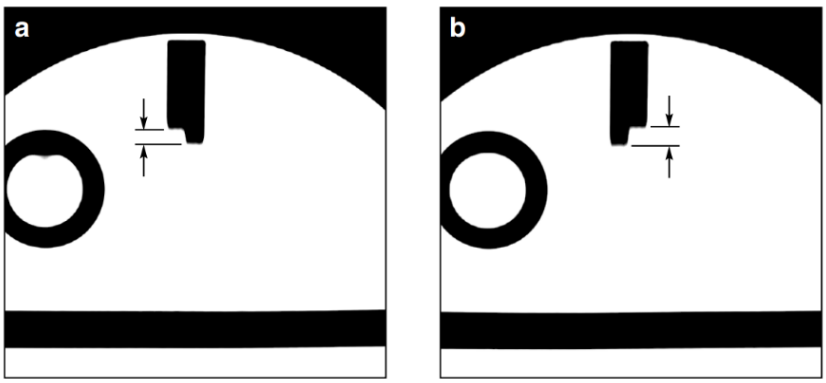

Figure B. 7 Images of slice 1 illustrating measurement of slice position error. The arrows indicate the bar length difference measurement that is to be made.

(a) The bar on the right is longer, meaning the slice is mispositioned superiorly; this bar length difference is assigned a positive value (+).

(b) The bar on the left is longer, meaning the slice is mispositioned inferiorly; this bar length difference is assigned a negative value.

Results

Table B. 6 Slice position accuracy test result

Series	Slice 1	Slice 11	Result
ACR T_1	+1.01	+1.37	Pass
ACR T_2_TE 20	+1.54	-0.79	Pass
ACR T_2_TE 80	+1.00	-1.00	Pass
Clinical T_1	+1.49	-0.75	Pass
Clinical T_2	+0.83	-1.38	Pass

Recommended Action Criteria: The magnitude of each bar length difference should be less or equal to 5mm.

Comment: PASS

5. Image intensity uniformity

Purpose: To measures the uniformity of the image intensity over a large water-only region of the phantom lying near the middle of the imaged volume and thus near the middle of the head coil

Method:

1. Display slice location 7.
2. Place a large, circular region-of-interest (ROI) on image. This ROI should have an area of between 195 cm^2 and 205 cm^2.
3. Set the display window to its minimum, and lower the level until the entire area inside the large ROI is white.
4. Measure low signal value as shown in Figure B.8 (b) by place the small ROI roughly 1 cm^2 at the region of dark pixels develops inside the large ROI.
5. Record the mean pixel value for this 1 cm^2 ROI. This is the measured low-signal value.
6. Raise the level until all but a small, roughly 1 cm^2 region of white pixels remains inside the large ROI. This is the region of highest signal as shown in figure B.8 (a).
7. Record the average pixel value for this 1 cm^2 ROI. This is the measured high-signal value.

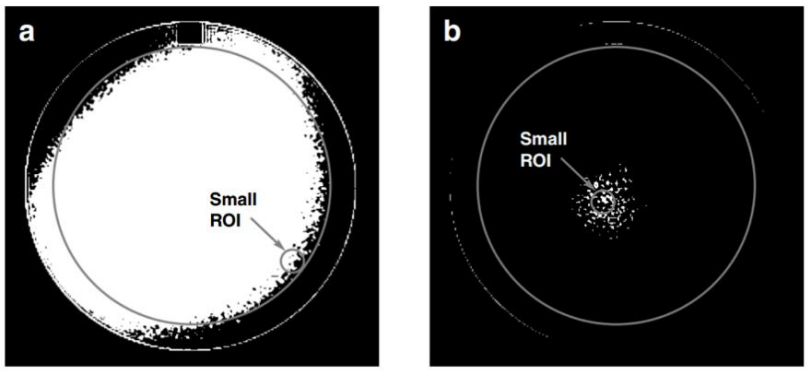

Figure B. 8 (b) ROI placement for low signal-value, (a) ROI placement for high signal-value.

The measured high-and low-signal values for each of the ACR series are combined to produce a value called percent integral uniformity (PIU). Use the following formula to calculate PIU:

$$PIU = 100 \times (1 - \{(high - low)/ (high + low)\})$$

Result*:*

Table B. 7 Image intensity uniformity test result

Series	Low signal	High signal	PIU (%)	Result
ACR T_1	961.46	934.48	98.58%	Pass
ACR T2_TE 20	1025.33	1050.9	98.10%	Pass
ACR T2_TE 80	504.61	475.74	97.06%	Pass
Clinical T_1	1005.73	985.89	99.00%	Pass
Clinical T_2	582.69	560.87	98.09%	Pass

Recommended Action Criteria: PIU should be greater than or equal to 87.5% for MRI systems with field strengths less than 3 Tesla.

Comment: PASS

6. Percent signal ghosting

Purpose: To assesses the level of ghosting in the image.

Method:

1. Display slice 7 of the ACR T1 series.
2. Using the workstation's ROI tool, 5 intensity measurements are made: Place a large ROI on the image an area between 195-205 cm^2, and the average intensity in the background at 4 locations outside of the image area of the ROI about 10 cm^2 as shown in figure B.9.

The value for the ghosting, as a fraction of the primary signal, is calculated using the following formula:

$$\text{Ghosting ratio} = \frac{(\text{top}+\text{btm})-(\text{left}+\text{right})}{(2\text{x}\text{Large ROI})}$$

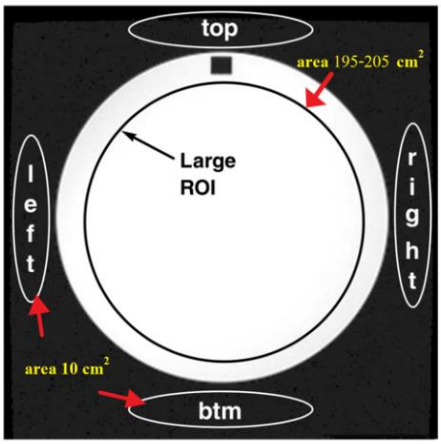

Figure B. 9 Image of slice 7 illustrating ROI placements for percent-signal ghosting measurements.

Table B. 8 Percent signal ghosting result

Series	Large	Top	Right	Left	Bottom	Calculated value	Result
ACR T_1	987.03	12.15	3.67	0.64	2.21	0.0053	Pass
ACR T_2_TE 20	1018.39	15.59	6.69	9.10	3.30	0.0017	Pass
ACR T_2_TE 80	444.43	15.17	4.39	6.70	1.49	0.0006	Pass
Clinical T_1	1034.56	21.57	7.86	12.08	3.74	0.0026	Pass
Clinical T_2	552.46	15.96	6.44	7.22	2.09	0.0039	Pass

Recommended Action Criteria: The ghosting ratio should be less than or equal to 0.025

Comment: PASS

7. **Low contrast object Detectability**

Purpose: To assesses the extent to which objects of low contrast are discernible in the images

Method:

The low-contrast objects appear on 4 slices: slices 8 through 11. In each slice the low-contrast objects appear as rows of small disks, with the rows radiating from the center of a circle like spokes in a wheel. Each spoke is made up of three disks, and there are ten spokes in each circle as show in Figure B.10. All the disks on a given slice have the same level of contrast. In order, from slice 8 to slice 11, the contrast values are 1.4%, 2.5%, 3.6%, and 5.1%. All the disks in a given spoke have the same diameter. Starting at the 12 o'clock position and moving clockwise, the disk diameter decreases progressively from 7.0 mm at the first spoke to 1.5 mm at the tenth spoke. The measurements for this test consist of counting the number of complete spokes seen in each of the four slices. This is done for each of the 4axial series.

Use the following procedure to score the number of complete spokes seen in a slice:

1. Display the slice to be scored. It helps to start with slice 11, which has the highest contrast objects.
2. Adjust the display window width and level settings for best visibility of the low-contrast objects.
3. Count the number of complete spokes and record the score.

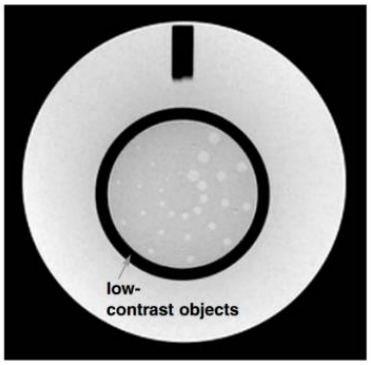

Figure B. 10 Image of slice 11 showing the circle of low contrast objects for the low-contrast object detectability test.

Result

Table B. 9 Low contrast detectability test result

Series	Slice 8	Slice 9	Slice 10	Slice 11	Total	Result
ACR T1	8	8	9	10	35	Pass
ACR T2_TE 20	8	10	10	10	38	Pass
ACR T2_TE 80	8	8	10	10	37	Pass
Clinical T1	4	8	10	10	32	Pass
Clinical T2	2	7	9	9	27	Pass

8. Image Artifact Evaluation

Table B. 10 Image artifact evaluation

Series	Excessive Ghosting		Excessive Truncation		RF Noise Leak		DC offset	
	Pass	Fail	Pass	Fail	Pass	Fail	Pass	Fail
ACR T1	✓		✓		✓		✓	
ACR T2_TE 20	✓		✓		✓		✓	
ACR T2_TE 80	✓		✓		✓		✓	
Clinical T1	✓		✓		✓		✓	
Clinical T2	✓		✓		✓		✓	

Recommended Action Criteria: For both in the ACR series and clinical series should have a total score of at least 9 spokes.

Comment: PASS

9. Magnet Visual Inspection

Table B. 11 Magnet visual inspection

Visual Inspection	Pass	Fail
RF door flange is present and door lock works properly	✓	
Patient alarm works properly	✓	
Magnet bore lights are working properly	✓	
Patient fan is working properly	✓	
Positioning lights are working properly	✓	
Patient table works properly	✓	
RF coils stored properly, cables are insulated, no visual defects	✓	
Patient/operator intercom system works properly	✓	
Daily QA system implemented	✓	
Operator's monitor is calibrated properly (SMPTE)	✓	
Images on film match display images (SMPTE)	✓	

Results Summary

Table B. 12 Medical physics phantom test results summary

TEST	Pass	Fail
Geometric Accuracy	✓	
High Contrast Spatial Resolution	✓	
Slice Position Accuracy	✓	
Slice Thickness	✓	
Image Uniformity	✓	
Signal to Noise Ratio	✓	
Low Contrast Detectability	✓	
Magnet Visual Inspection	✓	
Overall Phantom Test Results	✓	

Appendix C: T_2 Calculation method

In this study, T_2 were calculated using a nonlinear least-square curve fitting as a mono-exponential function. T_2 relaxation equation curve is as follows.

$$Y(TE) = M_0 \times e\,(-\frac{TE}{T_2})$$

Where M_0 is signal intensity from MR images in TE = 0 ms, TE is time of echo, T_2 is T_2 relaxation time

The Y(TE) of T_2-weighted images was modelled on an exponential decay with increasing TE as follows:

$$Y(TE) = Y_{TE=0} \times \exp(-\frac{TE}{T_2})$$

Where, $Y_{TE=0}$ is the SI at TE = 0, and the unknown coefficient is $Y_{TE=0}$ and T_2.

The following is the formula is deformed by the function of the natural logarithms.

$$\ln Y = \ln M_{O-}(\frac{TE}{T_2})$$

$$\ln Y = \ln M_{O-}(\frac{1}{T_2}) \times TE$$

Where, ln Y = Y, ln Mo = B and $1/T_2$ = A is assigned to the above function and it becomes the linear function equation.

$$Y = -A \times TE + B$$

Thus, T_2 is obtained in the form

$$T_2 = \frac{1}{A}$$

Appendix D: Consent form

	คณะกรรมการพิจารณาจริยธรรมการวิจัย คณะแพทยศาสตร์ จุฬาลงกรณ์มหาวิทยาลัย	เอกสารแสดงความยินยอมเข้าร่วมโครงการสำหรับอาสาสมัคร	AF 09-05/5.0 หน้า 1/2

การวิจัยเรื่อง การวัดค่า ทีทู (T_2 relaxation time) โดยใช้ ฮิสโตแกรมจากการวาด ROI ของกล้ามเนื้อ เพื่อการตรวจสอบการทำงานของกล้ามเนื้อ ในเครื่องถ่ายภาพสนามแม่เหล็กกำทอน 1.5 เทสลา

วันให้คำยินยอม วันที่.....เดือน.....พ.ศ.....

ข้าพเจ้า นาย/นาง/นางสาว.....

ที่อยู่.....ได้อ่านรายละเอียดจากเอกสารข้อมูลสำหรับผู้เข้าร่วมโครงการวิจัยวิจัยที่แนบมาฉบับวันที่..... และข้าพเจ้ายินยอมเข้าร่วมโครงการวิจัยโดยสมัครใจ

ข้าพเจ้าได้รับสำเนาเอกสารแสดงความยินยอมเข้าร่วมในโครงการวิจัยที่ข้าพเจ้าได้ลงนาม และ วันที่ พร้อมด้วยเอกสารข้อมูลสำหรับผู้เข้าร่วมโครงการวิจัย ทั้งนี้ก่อนที่จะลงนามในใบยินยอมให้ทำการวิจัยนี้ ข้าพเจ้าได้รับการอธิบายจากผู้วิจัยถึงวัตถุประสงค์ของการวิจัย ระยะเวลาของการทำวิจัย วิธีการวิจัย อันตราย หรืออาการที่อาจเกิดขึ้นจากการวิจัย รวมทั้งประโยชน์ที่จะเกิดขึ้นจากการวิจัย และแนวทางรักษาโดยวิธีอื่นอย่างละเอียด ข้าพเจ้ามีเวลาและโอกาสเพียงพอในการซักถามข้อสงสัยจนมีความเข้าใจอย่างดีแล้ว โดยผู้วิจัยได้ตอบคำถามต่าง ๆ ด้วยความเต็มใจไม่ปิดบังซ่อนเร้นจนข้าพเจ้าพอใจ

ข้าพเจ้ารับทราบจากผู้วิจัยว่าหากเกิดอันตรายใด ๆ จากการวิจัยดังกล่าว ข้าพเจ้าจะได้รับการรักษาพยาบาลโดยไม่เสียค่าใช้จ่าย

ข้าพเจ้ามีสิทธิที่จะบอกเลิกเข้าร่วมในโครงการวิจัยเมื่อใดก็ได้ โดยไม่จำเป็นต้องแจ้งเหตุผล และการบอกเลิกการเข้าร่วมการวิจัยนี้ จะไม่มีผลต่อการรักษาโรคหรือสิทธิอื่น ๆ ที่ข้าพเจ้าจะพึงได้รับต่อไป

ผู้วิจัยรับรองว่าจะเก็บข้อมูลส่วนตัวของข้าพเจ้าเป็นความลับ และจะเปิดเผยได้เฉพาะเมื่อได้รับการยินยอมจากข้าพเจ้าเท่านั้น บุคคลอื่นในนามของบริษัทผู้สนับสนุนการวิจัย คณะกรรมการพิจารณาจริยธรรมการวิจัยในคน สำนักงานคณะกรรมการอาหารและยาอาจได้รับอนุญาตให้เข้ามาตรวจและประมวลข้อมูลของข้าพเจ้า ทั้งนี้จะต้องกระทำไปเพื่อวัตถุประสงค์เพื่อตรวจสอบความถูกต้องของข้อมูลเท่านั้น โดยการตกลงที่จะเข้าร่วมการศึกษานี้ข้าพเจ้าได้ให้คำยินยอมที่จะให้มีการตรวจสอบข้อมูลประวัติทางการแพทย์ของข้าพเจ้าได้

ผู้วิจัยรับรองว่าจะไม่มีการเก็บข้อมูลใด ๆ เพิ่มเติม หลังจากที่ข้าพเจ้าขอยกเลิกการเข้าร่วมโครงการวิจัยและต้องการให้ทำลายเอกสารและ/หรือ ตัวอย่างที่ใช้ตรวจสอบทั้งหมดที่สามารถสืบค้นถึงตัวข้าพเจ้าได้

ข้าพเจ้าเข้าใจว่า ข้าพเจ้ามีสิทธิ์ที่จะตรวจสอบหรือแก้ไขข้อมูลส่วนตัวของข้าพเจ้าและสามารถยกเลิกการให้สิทธิในการใช้ข้อมูลส่วนตัวของข้าพเจ้าได้ โดยต้องแจ้งให้ผู้วิจัยรับทราบ

ข้าพเจ้าได้ตระหนักว่าข้อมูลในการวิจัยรวมถึงข้อมูลทางการแพทย์ของข้าพเจ้าที่ไม่มีการเปิดเผยชื่อ จะผ่านกระบวนการต่าง ๆ เช่น การเก็บข้อมูล การบันทึกข้อมูลในแบบบันทึกและในคอมพิวเตอร์ การตรวจสอบ การวิเคราะห์ และการรายงานข้อมูลเพื่อวัตถุประสงค์ทางวิชาการ รวมทั้งการใช้ข้อมูลทางการแพทย์ในอนาคตหรือการวิจัยทางด้านเภสัชภัณฑ์เท่านั้น

ข้าพเจ้าได้อ่านข้อความข้างต้นและมีความเข้าใจดีทุกประการแล้ว ยินดีเข้าร่วมในการวิจัยด้วยความเต็มใจ จึงได้ลงนามในเอกสารแสดงความยินยอมนี้

.....ลงนามผู้ให้ความยินยอม

(.....) ชื่อผู้ยินยอมตัวบรรจง

วันที่ .....เดือน.....พ.ศ.....

ข้าพเจ้าได้อธิบายถึงวัตถุประสงค์ของการวิจัย วิธีการวิจัย อันตราย หรืออาการไม่พึงประสงค์หรือความเสี่ยงที่อาจเกิดขึ้นจากการวิจัย หรือจากยาที่ใช้ รวมทั้งประโยชน์ที่จะเกิดขึ้นจากการวิจัยอย่างละเอียด ให้ผู้เข้าร่วมในโครงการวิจัยตามนามข้างต้นได้ทราบและมีความเข้าใจดีแล้ว พร้อมลงนามลงในเอกสารแสดงความยินยอมด้วยความเต็มใจ

.....ลงนามผู้ทำวิจัย
(.....) ชื่อผู้ทำวิจัย ตัวบรรจง
วันที่ .....เดือน.....พ.ศ.....

.....ลงนามพยาน
(.....) ชื่อพยาน ตัวบรรจง
วันที่ .....เดือน.....พ.ศ.....

Appendix E: Certificate of Approval of Institutional Review Board (IRB)

COA No. 676/2018

IRB No. 249/61

INSTITUTIONAL REVIEW BOARD

Faculty of Medicine, Chulalongkorn University

1873 Rama 4 Road, Patumwan, Bangkok 10330, Thailand, Tel 662-256-4493

Certificate of Approval

The Institutional Review Board of the Faculty of Medicine, Chulalongkorn University, Bangkok, Thailand, has approved the following study in compliance with the International guidelines for human research protection as Declaration of Helsinki, The Belmont Report, CIOMS Guideline and International Conference on Harmonization in Good Clinical Practice (ICH-GCP)

Study Title : The measurement of transverse relaxation time (T_2) using histogram from ROI setting in muscle activity study at 1.5 Tesla MRI

Study Code : -

Principal Investigator : Miss Kannikar Kanyakham

Affiliation of PI : Department of Radiology,
Faculty of Medicine, Chulalongkorn University.

Review Method : Full board

Continuing Report : At least once annually or submit the final report if finished.

Document Reviewed :

1. THESIS PROPOSAL Version 2.0 Date 29 June 2018
2. Protocol Synopsis Version 2.0 Date 2 July 2018
3. Information sheet for research participant Version 2.0 Date 1 July 2018
4. Informed consent for participating volunteers Version 2.0 Date 3 July 2018
5. Case Record Form: Phantom study Version 1.0 Date 29 March 2018

Approval granted is subject to the following conditions: (see back of this Certificate)

All approved investigators must comply with the following conditions:

1. Strictly conduct the research as required by the protocol;
2. Use only the information sheet, consent form (and recruitment materials, if any), interview outlines and/or questionnaires bearing the Institutional Review Board's seal of approval ; and return one copy of such documents of the first subject recruited to the Institutional Review Board (IRB) for the record;
3. Report to the Institutional Review Board any serious adverse event or any changes in the research activity within five working days;
4. Provide reports to the Institutional Review Board concerning the progress of the research upon the specified period of time or when requested;
5. If the study cannot be finished within the expire date of the approval certificate, the investigator is obliged to reapply for approval at least one month before the date of expiration.
6. If the research project is completed, the researcher must be form the Faculty of Medicine, Chulalongkorn University.

* A list of the Institutional Review Board members (names and positions) present at the meeting of Institutional Review Board on the date of approval of this study has been attached. All approved documents will be forwarded to the principal investigator.

6. Invitation to volunteer for the research project Version 3.0, 18 July 2018
7. Budget Version 1.0 Date 5 April 2018
8. Curriculum Vitae and GCP Training
   - Miss Kannikar Kanyakham
   - Assoc.Prof. Anchali Krisanachinda, Ph.D.
   - Prof. Noriyuki Tawara, Ph.D.

Signature .....
(Assistant Professor Apichai Vasuratna MD)
Vice-Chairman, Acting Chairman
The Institutional Review Board

Signature .....
(Associate Professor Onanong Kulaputana MD, PhD)
Member and Assistant Secretary, Acting Secretary
The Institutional Review Board

Date of Approval : July 26, 2018
Approval Expire Date : July 25, 2019

VITA

NAME	Kannikar Kanyakham
DATE OF BIRTH	09 March 1979
PLACE OF BIRTH	Roi-Et
INSTITUTIONS ATTENDED	Bachelor of Science Program in Radiological Technology, Mahidol University, 2002.
HOME ADDRESS	228/68 jw city condo rachada road, Chanhasem, Bangkok, Thailand 10900
PUBLICATION	-
AWARD RECEIVED	Best poster presentation Award 18 th Asia-Oceania Congress of a Medical Physics & 16 th South-East Asia Congress of Medical Physics. 11-14 November 2018 Kuala Lumpur, Malaysia.